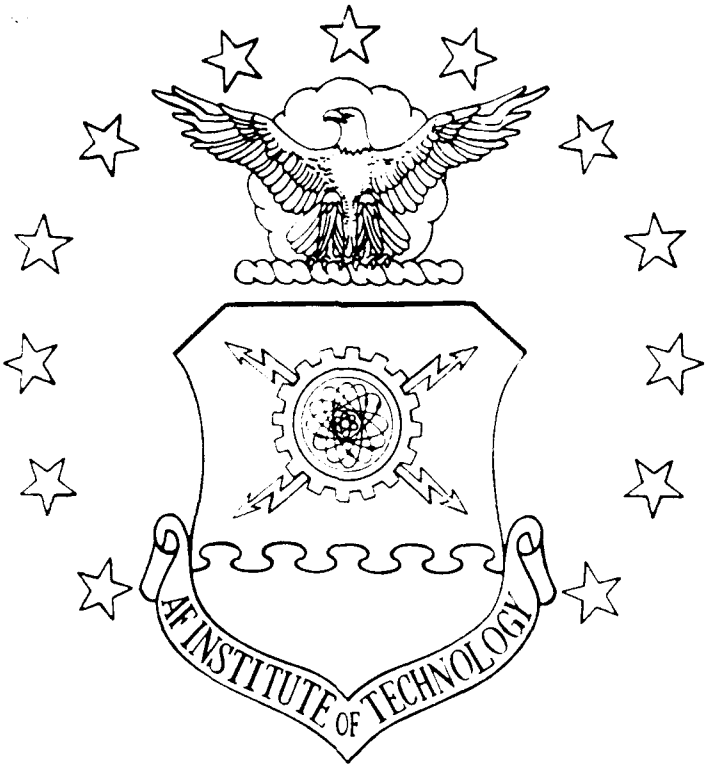

A COMPUTER MODEL OF A CO_2 OSCILLATOR—AMPLIFIER SYSTEM

THESIS

William Fredrick Anderson
Captain, USA

AFIT/GSO/ENP/90D-01

DEPARTMENT OF THE AIR FORCE
AIR UNIVERSITY
AIR FORCE INSTITUTE OF TECHNOLOGY

Wright-Patterson Air Force Base, Ohio

AFIT/GSO/ENP/90D-01

A COMPUTER MODEL OF A CO_2 OSCILLATOR—AMPLIFIER SYSTEM

THESIS

William Fredrick Anderson
Captain, USA

AFIT/GSO/ENP/90D-01

THESIS APPROVAL

STUDENT: Captain William F. Anderson CLASS: GSO 90-D

THESIS TITLE: A Computer Model of a CO_2 Oscillator—Amplifier System

DEFENSE DATE: 04 DEC 90

COMMITTEE:	NAME/DEPARTMENT	SIGNATURE
(Advisor)/co-Advisor (circle appropriate role)	Major David Stone/ENP	
(co-Advisor/ENS Representative) (circle appropriate role)	Major Michael Garrambone/ENS	
Reader	N/A	

AFIT/GSO/ENP/90D-01

A COMPUTER MODEL OF A CO_2 OSCILLATOR—AMPLIFIER SYSTEM

THESIS

Presented to the Faculty of the School of Engineering
of the Air Force Institute of Technology
Air University
In Partial Fulfillment of the
Requirements for the Degree of
Master of Science (Space Operations)

William Fredrick Anderson, B.S.
Captain, USA

December, 1990

Preface

The goal of this thesis was to design, develop and demonstrate an improved version of the Air Force Institute of Technology CO_2 laser amplifier model. The new model can be used as a laboratory design aid as well as an instructional tool in the classroom. This model provides valid data for graduate level studies in laser design. Since time is an important factor to practicing engineers and students alike, the model was constructed to be easy to learn and quick in operation.

The following chapters describe existing models which were used as a basis to build this model. The best features of these models were incorporated into the improved amplifier model. This thesis describes the validation of the improved model and includes a model user's guide as an appendix. It is assumed that the reader has had an introductory course in laser physics and will benefit from the brief presentation of the equations which form the foundation of the model.

I would like to thank my advisors, Dr. Stone and Major Garrambone, for their time and patience in helping me complete this project.

William Fredrick Anderson

Table of Contents

List of Figures

List of Tables

Abstract

An existing CO_2 laser amplifier simulation model developed for use on IBM-compatible personal computers has been improved through the redesign and addition of supplemental procedures from several models. The models and selected procedures which form the basis of the improved model are described. One procedure calculates the pumping rates of CO_2 and N_2 through calculation of the Boltzmann equation. Another procedure calculates the average vibrational temperatures of CO_2's vibrational modes. A third procedure replaces the Runge-Kutta integrator used in the original model with a faster, more accurate Adams-Bashforth-Moulton predictor-corrector integrator. Model validation for special conditions along with sample output is then presented. A user's guide is attached as an appendix.

The model allows students and designers to vary several input parameters to investigate the performance of the amplifier under various conditions. Parameters such as the cavity length, gas mix within the cavity, temperature, and pressure can be manipulated by the user in order to determine their effect on amplification.

A COMPUTER MODEL OF A CO_2 OSCILLATOR—AMPLIFIER SYSTEM

I. Background

1.1 Purpose

The purpose of this investigation was to produce and validate an improved version of an existing amplifier model and make it compatible with an upgraded version of an oscillator model currently in use at The Air Force Institute of Technology (AFIT). The following pages describe the importance of research in this area and previous work done at the Air Force Institute of Technology.

This model was designed to be used as a laser amplifier model which receives output from an existing laser oscillator model. This model can be used independently of an oscillator model, but was specifically developed to model the amplification of output from a laser oscillator model developed at The Air Force Institute of Technology. This chapter begins with a brief discussion of the significance of CO_2 (carbon dioxide) lasers and their applications. Next, models which were used as a basis for development of this model are described. Finally, the scope of the project is outlined.

1.2 Carbon Dioxide Laser Significance and Applications

Dr. A. L. Schawlow described lasers as, "an invention in search of an application" (10:1). Lasers have indeed been given many applications since their invention over thirty years ago. Laser applications today include carrying digital information in signal communications, cutting materials and tissue in industry and medicine, and determining the velocity of moving objects. There is a large variety of laser types.

The gas, doped insulator, semiconductor, and dye lasers are some examples of common lasers in use today. Each laser type has its own benefits and disadvantages.

The CO_2 laser is particularly interesting because of its impressive power and efficiency characteristics. W. J. Witteman, in his book *The CO_2 Laser*, states,

> The large interest in CO_2 lasers can also be understood from the fact that the efficiency of conversion of electrical energy into laser radiation combined with the maximum available power or pulse energy is by far superior to that of other laser systems ... CO_2 lasers have generally proven to be very versatile, simple to operate, and relatively cheap on investment and maintenance. (16:1)

CO_2 lasers produce a powerful, monochromatic, coherent beam of light at a wavelength of 10.6 micrometers. At this wavelength, the CO_2 laser has relatively high output power (compared to other lasers) at almost 30% efficiency (power out/power in). Consequently, CO_2 lasers have the greatest potential for use in industry and space, or any other environment which requires a system with a high power to weight ratio.

One application of the CO_2 laser is as a component of a space-based laser radar system. Laser radar systems in a space environment must be able to project a pulse of energy thousands of kilometers, yet be small enough to conform to bulk and weight constraints associated with placing a payload in orbit; therefore, considerable research is being conducted in space based laser applications. Dezenberg writes,

> The evolution of high velocity resolution CO_2 laser radars from the laboratory to airborne platforms ... to space platforms ... necessitates investigations of techniques to maintain high frequency stability operation of lasers in dynamic environments. (2:2)

SDI requires a system which can track and engage multiple targets with pinpoint precision. The CO_2 laser radar system is a likely candidate for performing this task as part of a global missile defense system.

1.3 Previous Models

The model described in this thesis was developed as a continuance of the work done within the Department of Physics at the Air Force Institute of Technology. The model makes extensive use of the results achieved by Dr. David Stone, Captain David Honey and Captain Frank Gallagher. Stone supervised the overall effort to develop models of a carbon dioxide laser oscillator and amplifier using the QuickBASIC programming language.

1.3.1 Stone's Oscillator Model. Dr. David Stone, a professor in the Department of Physics at the Air Force Institute of Technology, developed a computer model of a CO_2 laser oscillator. The model was written in QuickBASIC for use on IBM compatible personal computers. It is intended for use by graduate students as an instructional tool; it can also be used as a design aid in the laboratory. The model allows the designer to quickly predict laser oscillator output using any convenient personal computer.

The purpose of an oscillator in a laser radar system is to create a stable beam which maintains the constant wavelength (stable frequency) necessary for velocity determination using doppler radar principles. A wave with a stable frequency and acceptable signal to noise ratio can only be produced by *low* power oscillators, but unfortunately, a laser pulse from such an oscillator does not have enough power to produce a significant return from a distant target. Hence, an oscillator is used to create a very stable beam which is then amplified by a laser radar amplifier to the required power level. The result of an oscillator-amplifier pair is a stable, powerful beam of energy that can be used in a laser radar system (see Figure 1.1). Reilly writes,

> Laser radar oscillators must be short length and/or low pressure to obtain single longitudinal and single transverse mode (hence, single frequency) operation. Injection initiated oscillators can be used to obtain higher

powers, but waveform diversity and frequency are limited. Master oscillator power amplifier configurations overcome these limitations ... There are, however, other techniques to achieve high power frequency stable CO_2 laser radiation ... the laser amplifier is at present the technique of choice for the production of high power, high stability, CO_2 laser output. (12:60-61)

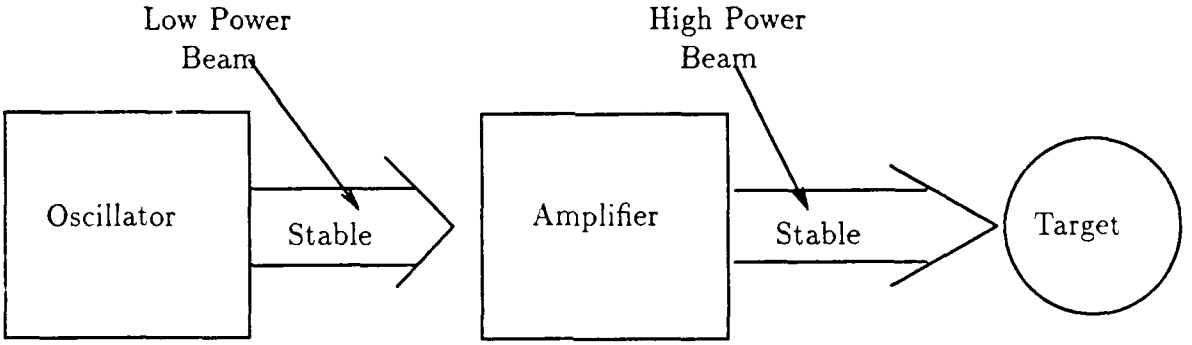

Figure 1.1. Oscillator-Amplifier Pair

Stone constructed his oscillator model using the work done by Gilbert. Rate equations which mathematically describe the physical processes of the laser were solved through Runge-Kutta integration. Gilbert *et al* modeled the kinetics of a CO_2 laser by means of a set of nonlinear rate equations idealized to a four-energy-level system (5:2523). Gilbert developed the model to describe "the fundamental dynamics of the active medium following excitation by short current pulses..." (5:2523). Gilbert used the energy diagram developed by Moore *et al* (8) (Figure 1.2) to develop the laser equations for his mathematical model. As Figure 1.2 shows, the CO_2 laser is modeled as a four level system. CO_2's three molecular vibrational modes ($\nu 1$, $\nu 2$, $\nu 3$) are shown in the model as 100 ($\nu 1$), 010 ($\nu 2$), and 001 ($\nu 3$). Nitrogen's vibrational energy ($\nu = 1$) level is very close in magnitude to the CO_2 (001) level and is used to transfer its vibrational energy to CO_2 molecules. N_2 is easily excited by electron pumping and transfers its energy to the CO_2 ($\nu = 3$) vibrational level. Lasing action occurs as CO_2 relaxes from the (001) energy level to the (100)

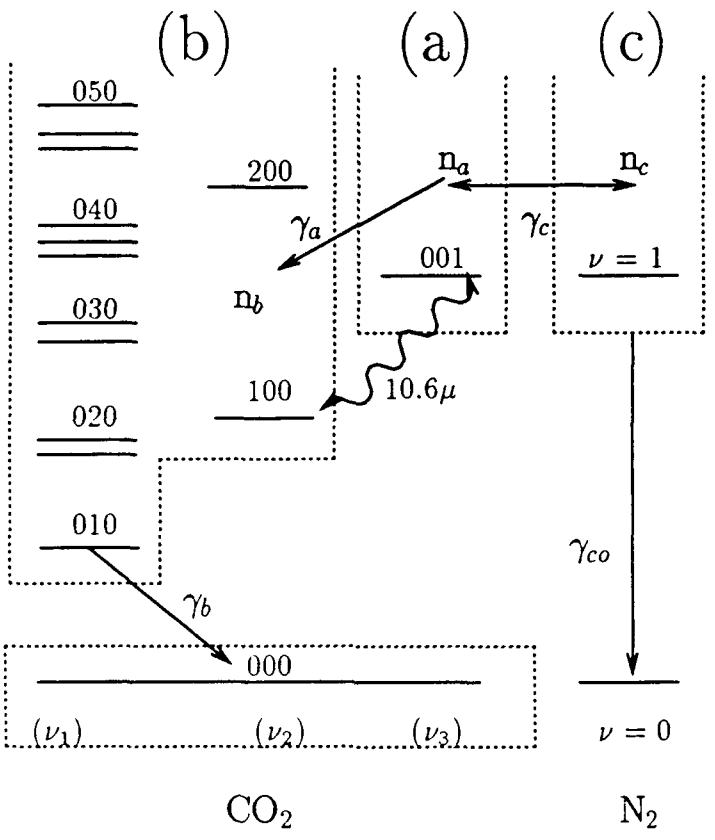

Figure 1.2. Moore's CO_2 Laser Transition Diagram (8)

energy level. Gilbert derived three equations which describe the time variation of the population in each level. Each equation describes the time rate of change of the population density of each group where group (a) represents the (001) level of CO_2, group (b) represents the (100) level of CO_2, and group (c) represents the $\nu = 1$ level of N_2 (see Figure 1.2). Gilbert's equations are as follows (5:2525):

$$\dot{n_a} = I\sigma_e c(n_b - n_a) - \gamma_a n_a + \gamma_c(n_c - n_a) + w_a \tag{1.1}$$

$$\dot{n_b} = I\sigma_e c(n_a - n_b) + \gamma_a n_a - \gamma_b n_b + w_b \tag{1.2}$$

$$\dot{n_c} = \gamma_c(n_a - n_c) - \gamma_{co} n_c + w_c \tag{1.3}$$

Gilbert included a fourth equation which describes the reaction of the laser medium on the photon density. The fourth equation is written as follows:

$$\dot{I} = -\gamma_o I + I\sigma_e c(n_a - n_b) + n_a w_s \tag{1.4}$$

The terms in the equations shown above are defined in the table below (5:2524-2525).

Symbol	*Meaning*
n_a	The population density of CO_2 molecules in the upper laser level.
n_b	The population density of CO_2 molecules in the lower laser level.
n_c	The population density of N_2 molecules in their $\nu = 1$ excited state.
$I\sigma_e c$	Rate coefficient for stimulated emission or absorption.
γ_a,γ_b,γ_c, γ_{co}	Kinetic rate constants. γ_a, γ_b, and γ_{co} relate to the collisional deactivation of the initial (a) and terminal (b) laser levels. γ_c describes the transfer of energy from excited N_2 to the (001) ($\nu = 3$) level of CO_2 and vice versa.
w_a,w_b, w_c	Pump terms describing the rates at which the respective laser levels are excited during the electrical discharge pulse.
w_s	Spontaneous emission rate on the longitudinal mode of the laser.
γ_o	Reciprocal of the decay time of the photon population I in the cavity (1/tcav).
I	Radiation density (photons/cm^3).

Gilbert simplifies the model by assuming constant values for all terms except for the number densities (n_a, n_b, and n_c). While this may seem unrealistic at first, the output of his model agrees with the results for preselected experimental conditions. Gilbert assumes reasonable values for the parameters of a specific laser hardware configuration (N_2, He, and CO_2 gas mix, cavity pressure, etc.). Gilbert's model

is valid only for preselected experimental conditions and cannot be used to model systems with other nonconstant parameter values.

Stone used the same rate equations shown above, but did not assume constant values for γ_a, γ_b, γ_c, or σ_e. The values for these terms are calculated by his program depending on the pressure and gas mix ratios selected by the person using the model. Stone used the following rate equations in his oscillator model:

$$\dot{n_a} = I\sigma_e c\,(\frac{g_a}{g_b}\,n_b - n_a) - \gamma_a n_a + (\gamma_{CO2}\,n_c - \gamma_{N2}\,n_a) + w_a \tag{1.5}$$

$$\dot{n_b} = I\sigma_e c\,(n_a - \frac{g_a}{g_b}\,n_b) + \frac{1}{4}\gamma_a n_a - \gamma_b n_b + w_b \tag{1.6}$$

$$\dot{n_c} = \gamma_{N2}\,n_a - \gamma_{CO2}\,n_c + w_c \tag{1.7}$$

$$\dot{I} = I\sigma_e c\,(n_a - \frac{g_a}{g_b}\,n_b - 1 - \alpha) + w_s\,n_a \tag{1.8}$$

where

I = Photon density in the laser cavity
γ_{N2} = Collisional relaxation rate for N_2 based on the % CO_2 in the gas mix
γ_{CO2} = Collisional relaxation rate for CO_2 based on the % N_2 in the gas mix
w_s = Spontaneous emission rate in the cavity
g_x = The degeneracy ratio of level x (16:15).
α = The unfavorable losses in the cavity due to absorption

Stone also included the ability to model both ^{12}C and ^{13}C based CO_2 lasers. By including the γ and σ_e terms as variables (not constants), Stone's model more accurately serves the user by allowing him to vary the characteristics of the laser hardware. Thus, the model's output is valid for modeling CO_2 lasers with variable gas ratios, cavity pressures and temperatures.

Stone's program asks the user for numerous input parameters such as the temperature, gas mix (percent CO_2, N_2, He, H_2O, and H_2), length of the cavity, and

laser pulse length (in time) and predicts the characteristics of the output laser pulse. The program uses the Adams-Bashforth-Moulton integration method to numerically solve the rate equations. Stone's model uses the Boltz procedure written by Honey to calculate the pump terms shown in the rate equations. Stone's model predicts the general behavior of a laser oscillator with given input parameters.

Stone supervised additional work with carbon dioxide laser models as the thesis advisor to two graduate students. Honey worked independently to improve Stone's existing oscillator model while Gallagher developed an amplifier model which could be used separately or in conjunction with Stone's model. The intent remained to produce models which could be used on IBM compatible personal computers in the classroom or laboratory. Each model was written in QuickBASIC to maintain project consistency.

1.3.2 Honey's Improved CO_2 Laser Oscillator Model. Honey's contribution to Stone's work was the development of a procedure that more accurately determines the values of the pumping terms (w_a, w_b, w_c) used in equations (5), (6), and (7) shown above. An initial version of Stone's model calculated the pump rates based on an assumption of the pump efficiency. Honey's procedure numerically solves the Boltzmann equation in order to compute more accurate values of the pump terms.

The laser is pumped by the collision of electrons with N_2 and CO_2. N_2 is easily excited and decays only through collisions with the cavity walls or CO_2 molecules. Wittemann writes,

> It has been observed that an electric discharge in nitrogen leads to a very effective formation of vibrationally excited N_2 molecules .... Since the N_2 molecule has two identical nuclei, its dipole radiation is forbidden. It can only decay by collisions with the wall of the containing vessel or by collisions with other molecules. (16:64)

Since the N_2 $\nu = 1$ and CO_2 (001) energy levels have an energy difference of only 18 cm^{-1}, N_2 readily transfers its energy to CO_2 and relaxes down to the ground state. CO_2 is also directly pumped by collisions with electrons. CO_2 in the ground state is thus pumped to the (001) level both by collision with excited N_2 molecules in the $\nu = 1$ energy level and with free electrons in the applied electric field.

N_2 and CO_2 cannot be pumped to the desired energy levels by collision with any electron; they must collide with an electron that has an energy level (velocity) equal to or greater than the N_2 $\nu = 1$ or CO_2 (001) energy level. This minimum energy can be found using the following equation for energy:

$$E = h\nu \tag{1.9}$$

where

E = The energy of the vibrational level (joules)
h = Planck's constant (6.6260755 x 10^{-34} joules · seconds)
ν = The characteristic frequency of the energy level ($seconds^{-1}$)

For the N_2 $\nu = 1$ energy level, E is approximately 4.7602 x 10^{-20} joules. The velocity of an electron with this energy can be derived from the equation for kinetic energy:

$$E = \frac{1}{2}mv^2 \tag{1.10}$$

where

E = The energy of the electron (joules)
m = The mass of an electron (9.1093897 x 10^{-31} kg)
v = The velocity of the electron (meters per second)

Solving for velocity and substituting the energy calculated above, the critical velocity is 3.23 x 10^5 meters per second. Electrons with this velocity have enough

energy to pump the CO_2 and N_2 molecules. Also, an electron with a higher energy level (velocity) can transfer a portion of its energy and pump CO_2 and N_2. Therefore, only a fraction of the electrons in the laser cavity will have velocities suitable for pumping. Wittemann (reference (16)) provides an excellent description of electron pumping and its effect on the laser medium. Honey determined the velocity distribution of the electrons in the applied field for a given parameter set ($\frac{E}{N}$, ambient gas temperature, etc.). He used the Boltzmann equation to "relate ... these various factors and ...[compute] the electron number density as a function of the velocity (or energy) (7:2)."

The Boltzmann equation considers the force of the electric field on the electrons and their subsequent collisions with gas molecules within the laser cavity. Honey assumes that the electron mean free path is small compared to the size of the laser cavity, resulting in a spherically symmetric electron velocity distribution (7:2). Energy is transferred by electrons to CO_2 and N_2 gas molecules through elastic collisions, the applied electric field, and inelastic collisions. A detailed analysis of the energy transfer through collisions and the applied electric field is given in Chapter 2 of Honey's thesis (7:3-16).

Honey's procedure inputs several parameters, calculates the electron number density distribution, and outputs the pump rates. A simplified flow chart of the procedure (named "Boltz") is shown in Figure 1.3.

Boltz makes use of ten parameters from the main body of the oscillator code. These ten parameters are used to calculate the electron number density distribution leading to the output of the pump terms w_a, w_b, and w_c. These parameters are listed below (7:17-19).

1. kc - the number of cells or bins into which the energy axis has been divided as a result of finite differencing
2. de - width of a bin in electron volts

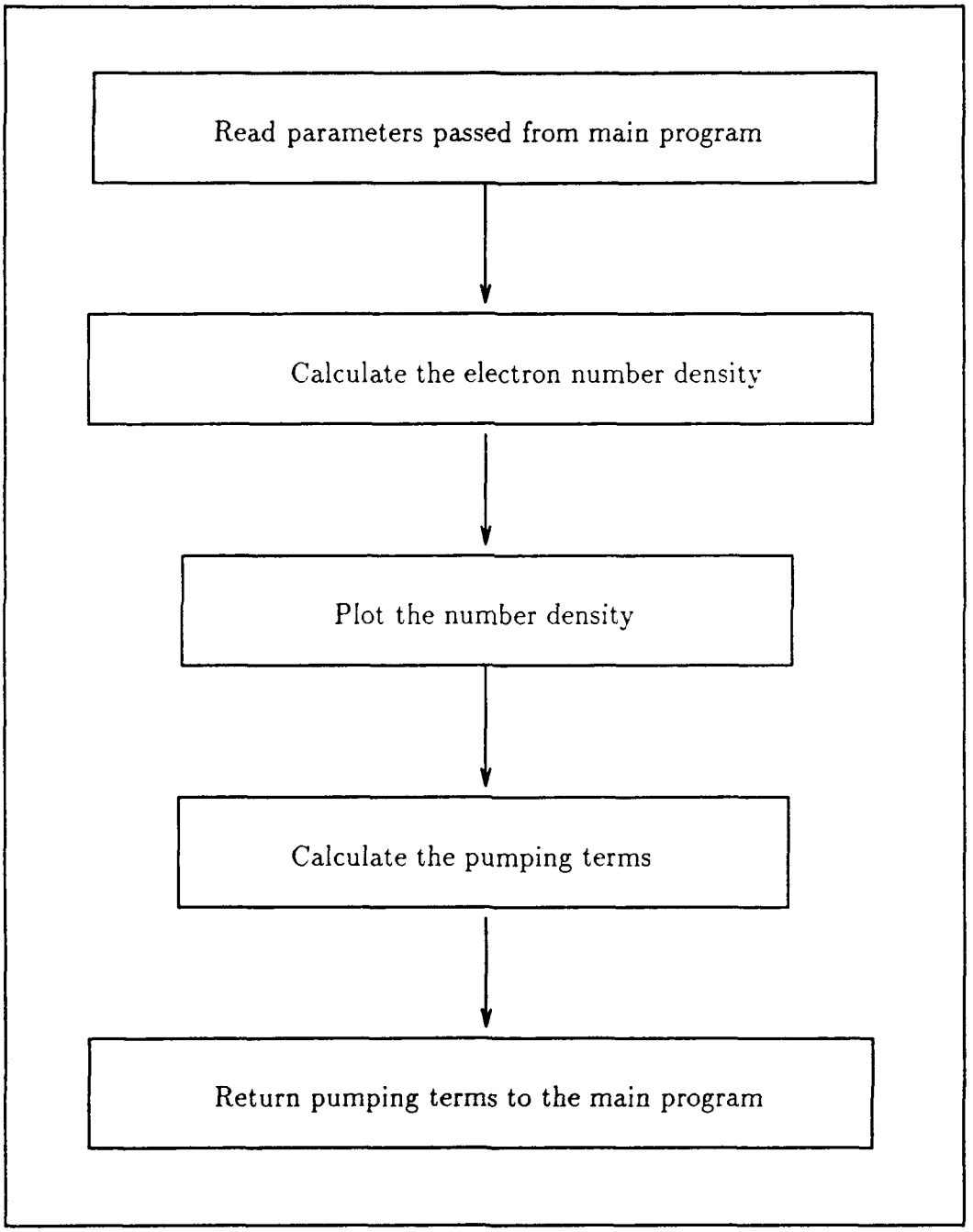

Figure 1.3. Honey's Boltz Procedure Flow Chart

3. pres - total pressure of the gas mixture in atmospheres
4. d2 - percentage of CO_2 in the gas mix
5. d1 - percentage of N_2 in the gas mix
6. d3 - percentage of He in the gas mix
7. T - ambient temperature of the gas mix
8. VT() - a three element vector containing the vibrational temperatures for the (010), (100), and (001) states of CO_2
9. EN - E/N, the electric field strength (volts/centimeter) divided by the gas number density
10. jd - currrent density in the plasma tube (amps/centimeter^2)

1.3.3 Gallagher's Amplifier Model. Gallagher modeled a CO_2 laser radar amplifier. The model can be used to investigate the amplification of either square input pulses or pulses generated with a laser oscillator. Like Stone's and Honey's models, Gallagher's model allows manipulation of several input parameters such as cavity length and diameter, gas mixture, temperature, pressure, window reflectivity, and pump efficiency (4:ix). Gallagher's model essentially analyzes amplifier gain as the pulse travels down the length of the amplifier. The model also describes the effects of amplified spontaneous emission and its effect on the output pulse.

An amplifier in an oscillator-amplifier scheme is essentially a gas filled container in which a population inversion exists. The output pulse of the oscillator is directed into the amplifier. Incoming photons from the oscillator strike excited atoms in the amplifier and the result is a gain in the photon flux and degradation of the population inversion. Longitudinally, the photon flux grows and the population inversion is reduced as the input beam travels down the amplifier. This is called a single pass amplifier since the beam enters one end of the amplifier and exits the other without reflection.

Gallagher modeled the amplifier as a one dimensional system. He assumed constant inversion and flux across the width (cross-section) of the amplifier. Gallagher also assumed the diameter of the input beam to be equal to the diameter of the amplifier (4:2-1). He accounted for the fact that the leading photons of the input oscillator pulse will experience a greater population inversion than those at the end of the pulse.

Gallagher divided the amplifier into a number of cells and tracked the progress of the input beam as it moves from cell to cell. The number of cells in the amplifier is determined by the amplifier's length, the basic time unit (tcav), and the integration time step (h1).

Since Gallagher's model supplements Stone's model, Gallagher, like Stone, used the average lifetime of a photon in the laser cavity as the basic time unit (tcav). The integration process uses a time step (h1) to determine values at selected fractions of the basic time unit. For example, if the cavity lifetime is selected as tcav = 20 nanoseconds and the integration time step h1 = .1, then the integration process is executed every 2 nanoseconds (20 x .1). Using the speed of light in the laser medium (approximately 3 x 10^8 meters/second), the cell width for this time step is 2 nanoseconds x (speed of light) or .6 meters. If the cavity length selected by the operator is 1.2 meters, then the program divides the laser into 2 cells. In order for Gallagher's code to use an output pulse from Stone's oscillator code, Gallagher's model must receive the values of tcav and h1 that were used by the oscillator code to generate the input pulse.

Gallagher's method for calculating the pumping terms was taken from an early version of Stone's oscillator model. The method was based on an assumed pump efficiency of the system. The operator interfacing with the model inputs the pump efficiency for the oscillator being modeled. The user must use realistic values for the pump efficiency in order for the model to calculate reasonable pumping terms. Stone's equations (used by Gallagher) for the pump terms are shown below.

$$w_a = \frac{1}{3}\eta_{pump} N_{CO_2} \frac{1}{t_{pp}} \quad (1.11)$$

$$w_b = w_a \quad (1.12)$$

$$w_c = \eta_{pump} N_{N_2} \frac{1}{t_{pp}} \quad (1.13)$$

where

η_{pump} = Pump efficiency. Pump efficiency is the fraction of N_2 molecules pumped to the ν =1 energy level.

N_{CO_2} = Number density (per meter^3) of CO_2 molecules in the gas mix in the laser cavity.

N_{N_2} = Number density (per meter^3) of N_2 molecules in the gas mix in the laser cavity.

t_{pp} = Duration of the pump pulse (nanoseconds).

Stone assumed that CO_2 molecules are pumped at the same rate to the (001) and (100) energy level. While these are valid assumptions for different CO_2 oscillators with varying gas ratios, current densities, and E/N ratios, the calculated pump rates are only approximations. Honey's procedure more accurately calculates the pump rates by numerically solving the Boltzmann equation.

Gallagher used the Runge-Kutta integration method to calculate the number densities of CO_2 (001), CO_2 (100), and N_2 ($\nu = 1$) atoms in the laser medium. Equations (5), (6), and (7) are solved numerically to determine the population inversion within the cavity for a given time step for a given cell. The flux, or photon density, is calculated outside the rate equations using equation (15) shown below. The value for the inversion leads to determination of the amplifier gain.

The gain coefficient (g) is the product of the population inversion and the stimulated emission cross section (4:2-4). The population inversion is simply the difference between the number densities of the CO_2 (001) and CO_2 (100) number densities expressed as n_a - (degeneracy ratio) $\cdot$ n_b. Values for n_a and n_b are determined by the Runge-Kutta integration procedure applied to equations (5) through

(7). The stimulated emission cross section, σ, is calculated by the equation shown below (4:2-4).

$$\sigma = \frac{F_{u(J=19)}(A_{21})c^2}{4\pi(\nu^2)\Delta\nu_p} \tag{1.14}$$

where

A_{21} = The Einstein coefficient for spontaneous emission

ν = The characteristic frequency of the $J19$ - $J20$ [$P(20)$] transition

$\Delta\ \nu_p$ = The linewidth of the emission

$F_{u(J=19)}$ = The fraction of molecules in the (001) vibrational level that are in the ($J = 19$) rotational level

The gain coefficient ($g = (n_a - n_b) \cdot \sigma$) is the key to the determination of the amplifier system gain applied to the input pulse.

Gallagher used a single amplifier equation to model the photon density growth from cell to cell. The equation below describes this growth from a particular time (j) and cell (k) to the next time (j + 1) and cell (k + 1).

$$P_{(j+1,k+1)} = P_{(j,k)}e^{(g_{(j,k)}-\alpha)L} \tag{1.15}$$

where

P = Number of photons per meter^3

g = Gain coefficient

α = Loss per unit distance due to scattering and absorption

L = Length of the amplifier cell

Gallagher also considered the effects of amplified spontaneous emission. Amplified spontaneous emission occurs when the population inversion within the amplifier

cavity emits photons as some excited atoms spontaneously relax to lower energy levels. These photons strike excited atoms in the inversion causing stimulated emission. Since spontaneous emission can occur between a large number of rotational energy levels, the energy loss from spontaneous emission is counterproductive to amplifier performance. As stated earlier, precise frequencies are essential to laser radar. The objective of an oscillator-amplifier system is to amplify precise, low power oscillator output. Spontaneous emission at multiple frequencies degrades the performance of the oscillator-amplifier system.

The amplifier model flow chart is shown in Figure 1.4. Since this thesis uses Gallagher's model as its foundation, a detailed description of his model is presented here with each portion of the flow chart (Figure 1.4) being described in the following paragraphs.

Display menu to the user. The model asks the user whether the amplifier model will be used to amplify a pulse generated by Stone's oscillator code or if the user desires to amplify a square pulse generated by the amplifier model. If the square pulse option is chosen, the amplifier model creates a square (constant amplitude) input pulse with a magnitude chosen by the user. The operator can further choose to manipulate numerous parameters which affect the amplification of the input pulse or allow default parameters to establish the initial conditions. The parameters the user can alter are listed in Table 1.1.

Calculating collisional relaxation rates. The rate at which molecules relax due to collisions within the gas mix in the laser cavity is described by the γ_a, γ_b, γ_c, and γ_{co} terms in the rate equations (equations (1.1) - (1.3)). Gallagher used Stone's equations for calculating these terms. The rates are dependent on the gas mix (percent CO_2, N_2, He, and H_2O), cavity pressure, and type of carbon isotope (^{13}C or ^{12}C).

Calculating the number density of the gas mix. The number density (N) of all molecules in the cavity is dependent on the pressure (P) and temperature (T). The

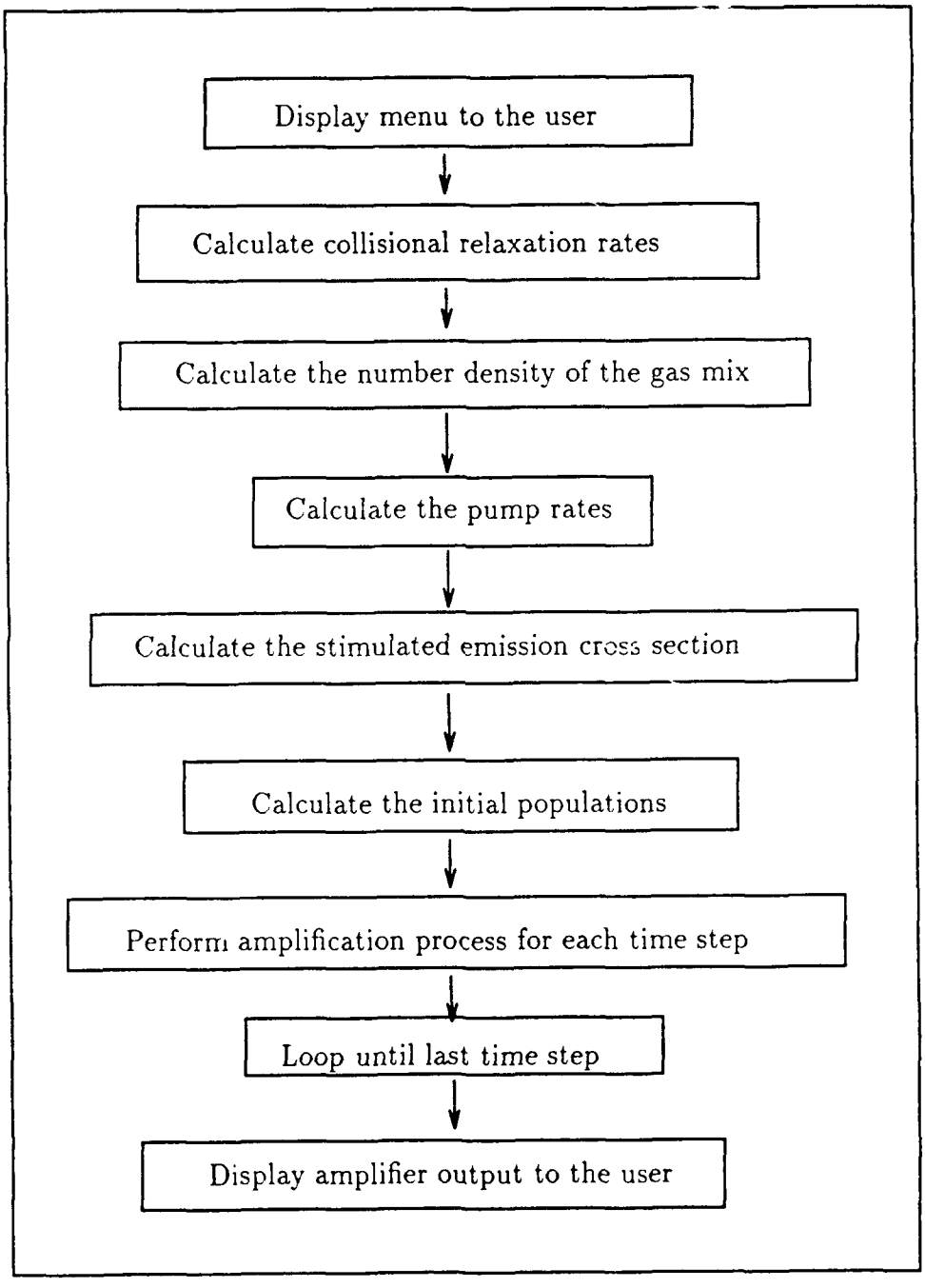

Figure 1.4. Amplifier Model Flow Chart

Table 1.1. Amplifier Model Parameters

Parameter Name	*Description*
h1	Integration time step
diameter	Input beam diameter
length	Amplifier length
pres	Pressure in atmospheres
pctCO2	Percent CO_2 in the gas mixture
pctN2	Percent N_2 in the gas mixture
pctHe	Percent He in the gas misture
pctH2O	Percent H_2O in the gas misture
temp	Temperature of the gas mixture
taupump	Length (nsec) of the pump pulse
delay	Delay (nsec) before pump pulse begins
alpha	Loss per unit length due to scattering or absorption
reflection	Coupling loss term
ASEflag	Operator chooses whether or not to consider ASE losses

following equation is used to calculate the number density in molecules/meter^3 with k_B = Boltzmann's constant.

$$N = \frac{101320P}{Tk_B} \tag{1.16}$$

Under the conditions of 1 atmosphere and 300 °K, the number density is approximately 2.45 x 10^{25} molecules/meter^3.

Calculating the pump rates. Gallagher used Stone's method of calculating the pump rates described by equations (11) - (13). As explained above, the rates are good approximations.

Calculating the stimulated emission cross section. Gallagher used equation (14) to calculate the stimulated emission cross section. F_u is temperature dependent and $\Delta\nu_p$ is temperature and pressure dependent.

Calculating the initial population. The initial populations of the CO_2 (001), CO_2 (100), and N_2 ($\nu = 1$) energy levels are dependent on the temperature and percent gas mix. The initial number density of CO_2 molecules in the (001) energy level (n_{a_o}), is expressed by the following equation:

$$n_{a_o} = N(\frac{\%CO_2}{100})e^{\frac{-h\nu}{k_B T}} \tag{1.17}$$

where

N = Total number density
h = Planck's constant
ν = Characteristic frequency of the (001) energy level
k_B = Boltzmann's constant
T = Temperature of the gas mix (kelvin)

n_{b_o} and n_{c_o} are calculated in the same manner. This equation is only valid for low temperatures (a few hundred degrees kelvin).

Performing the amplification process. Amplifier gain is calcuated for each cell as the input pulse travels through the length of the amplifier. A Runge-Kutta integration procedure evaluates the rate equations and returns the values of n_a and n_b. The difference between n_a and n_b describes the inversion density. This quantity multiplied by σ determines the gain coefficient. The increase in photon flux is described by equation (15) which uses the gain coefficient and the length of the cell.

Loop until last time step. Amplifier gain and the resulting increase in photon density are computed for each cell for the entire duration of the run.

Display amplifier output to the user. Values recorded during each time step are displayed on output screens. The user can save files of populations, gains, and power values and return to the main menu to try another experiment.

Gallagher's model uses many components of Stone's model to simulate the behavior of a laser amplifier. Gallagher uses Stone's original Runge-Kutta integration procedure and method of computing the collisional relaxation rates and pump terms. Since Gallagher worked independently of Honey, he did not include the Boltz procedure for calculating the pump terms.

1.4 Scope

The scope of this project is limited to improving Gallagher's amplifier model in an effort to achieve more accurate output for a given input pulse. Improvement is gained through incorporation of existing procedures from Stone's and Honey's models and the inclusion of an Adams-Bashforth-Moulton integrator replacing the slower, less accurate Runge-Kutta integrator used in Gallagher's model.

This amplifier model calculates the pumping terms (w_a,w_b,w_c) using Honey's Boltz procedure. The model also uses Stone's method for computing the average vibrational temperatures for the (010), (100), and (001) states of CO_2. A major effort was exerted to make the code more flexible and readable by converting large portions of main body code into procedures. The procedures are better suited for further refinement and embellishment of the model.

Amplified spontaneous emission (ASE) is not addressed by this model. The ASE portions of Gallagher's model, combined with the Boltz procedure and temperature averaging embellishments, consume large amounts of computer memory. Since the goal is to produce a model with reasonable run times along with accurate output, ASE is not included in this model. The intent of this work is to produce output that can be used to validate the embellished amplifier model. For the purpose of this investigation, ASE losses add too much complexity to the validation process. ASE effects do not have a significant impact on model output (14).

II. Model Development

This chapter describes the work accomplished in order to construct the improved amplifier model. Gallagher's model was used as the framework and embellishments were added in the form of procedures and additions to the main body code. Microsoft's QuickBASIC version 4.5 was used as the programming language.

2.1 Gallagher's Code

Gallagher's original code (filename CO2AMP1) was modified in order to reduce memory requirements and make it compatible with the upgraded versions of Stone's oscillator code. The major changes involved the development of procedures to replace main body code and the alteration of several normalization constants.

In order to reduce memory requirements, redundant operations were eliminated or placed into a procedure. Gallagher's code has over 1000 lines, but only 5 procedures. This effort broke Gallagher's code into its major components. Each component was converted into a procedure which is called from a much smaller main body. The new procedures now make the code shorter and more readable. This amplifier model consists of over 22 procedures; some of the procedures are taken directly from Gallagher's code, while others support the embellishments discussed below.

2.2 Addition of Boltz Procedure

Honey's Boltz procedure was added to CO2AMP1 in order to calculate the pump terms used in the rate equations. Boltz replaces the pump rate approximations used in Gallagher's amplifier model. In order to merge Boltz with CO2AMP1, Boltz's 10 parameters (see section 1.3.2) had to be identified in the main program.

Boltz uses the ten parameters passed from the main program to compute the three pump terms, w_a,w_b, and w_c used by the rate equations in the amplifier model.

CO2AMP1 defined 5 of the 10 required parameters; 5 additional parameters had to be created specifically for use with the Boltz procedure. The pressure of the gas mixture, percentage of each gas in the mixture (CO_2, N_2, He), and the ambient temperature of the gases are defined in CO2MP1. The five remaining parameters were inserted into the main program and placed in the main menu for value assignment by the user. The 5 parameters are de, kc, VT() (an array), EN, and jd. Each parameter is explained below.

Parameter de. de represents the energy axis of the electron energy versus excitation cross section curves for CO_2 (see Figure 2.1). Figure 2.1 is a reproduction taken from reference (16:66) which provides a detailed explanation of electron energy and vibrational excitation cross sections. The figure shows that electrons with energies of approximately .5 eV will have the greatest chance of exciting CO_2 molecules into the (001) energy level. The probability that electrons with very high velocities (energies greater than 5 eV) will transfer the required energy is small. For this model, the energy axis is initialized at 5 eV. A product of de · kc equal to 5 eV is suitable for calculating the pump rates using Boltz.

Parameter kc. kc represents the number of energy bins or cells into which the energy axis has been divided. The value of kc provides the resolution of pump rate calculation. Boltz's internal dynamic arrays are dimensioned by kc. A higher value of kc leads to a more precise pump rate calculation. Boltz uses arrays as matrices to perform necessary calculations. At one point, the matrix is inverted. A value of kc = 50 means that a 50 x 50 array is used in matrix multiplication and inverted. A small increase in kc results in larger matrices, longer run times, and greater memory use. If a very large kc is chosen, the model can exceed memory capabilities and the program will fail. A value of kc = 30 provides quick and accurate results. Values over 50 are more accurate, but the run time can last several minutes. Values over 50 do not add enough accuracy to warrant the procedure's longer run time.

VT() array. The VT() array is passed to Boltz from the main program. VT(1),

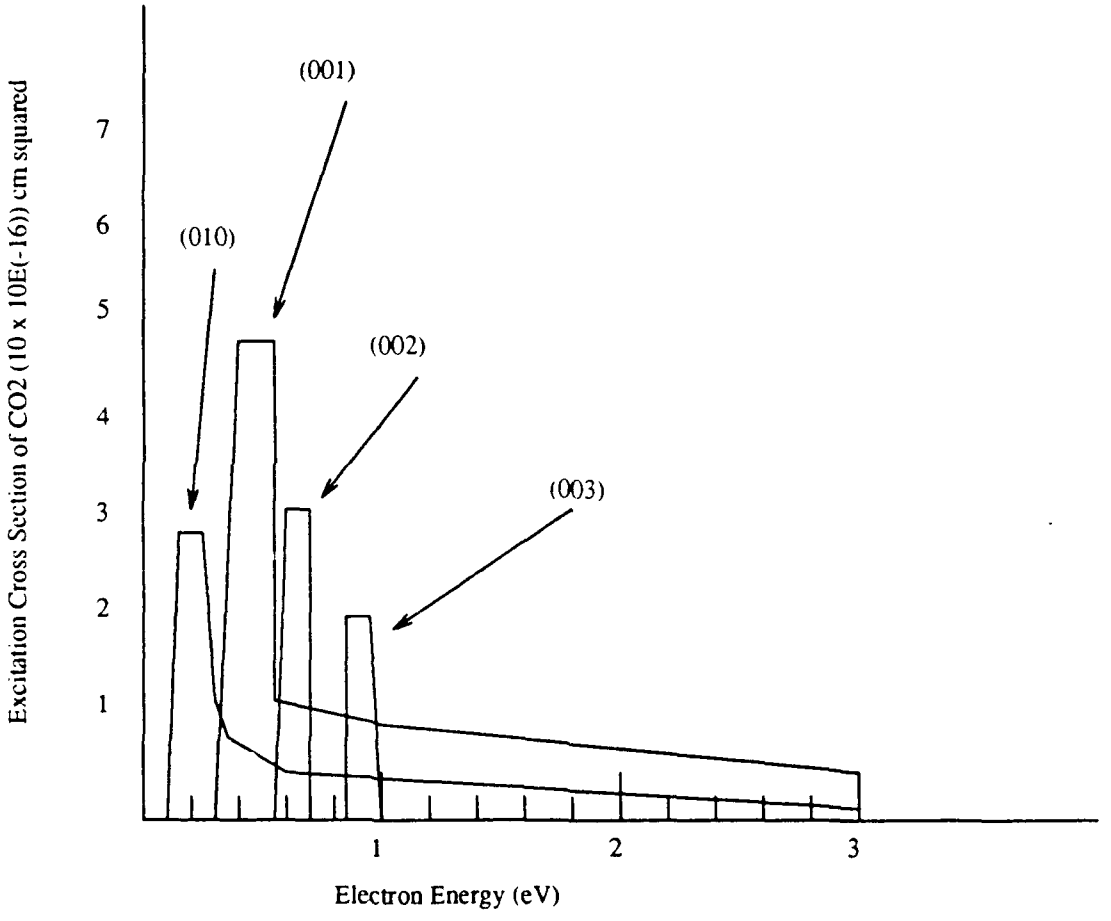

Figure 2.1. Cross Sections for Vibrational Excitation of CO_2 by Electron Impact

VT(2), and VT(3) represent the vibrational temperatures of CO_2's modes (100), (010), and (001), respectively. The vibration of a CO_2 molecule in each mode can be described by its temperature (16:68). Wittemann writes, "It is also expected that the $\nu 1$ and $\nu 2$ vibrations are in rapid equilibrium with each other because of the near-resonant process ..." (16:68). Since the (n00) and (0n0) vibrational temperatures are equal, this model sets the (100) vibrational temperature equal to the (010) vibrational temperature. The (001) level is not equal to (100) or (010) and maintains its own value. This model initially sets the values of VT(1) - VT(3) equal to 300. A section of Stone's oscillator code used to calculate the average vibrational temperatures of the (100) and (001) modes is included in the amplifier model and is discussed in the next section of this chapter.

Parameters EN and jd. EN represents the electric field strength (volts/cm) divided by the gas number density (molecules/cm^3). The units of EN are volts · cm^2. Parameter jd represents the current density in the plasma tube (amps/cm^2). The product of the two values represents the power applied to the cavity in an effort to pump the system. The energy loaded is displayed on the screen for the user in joules/liter and is derived from the equation below.

$$EnergyLoading = EN \cdot jd \cdot N \cdot taupump \cdot tcav \cdot 10^{-3} \tag{2.1}$$

where

EN = Electric field strength divided by the gas number density (volts · cm^2)
jd = Current density in the plasma tube (amps/cm^2)
N = Total number density of molecules in the cavity (meters^{-3})
$taupump$ = Pump time in cavity lifetimes
$tcav$ = cavity lifetime (seconds)

10^{-3} converts from (meters^{-3}) to (liters^{-1}). The total power is $EN \cdot jd \cdot Ndensity \cdot 10^{-3}$ (joules)/(liter · seconds). The total pump time is $taupump \cdot tcav$ (seconds). Total power x total pump time yields total energy loading (joules/liter).

A change in the value of any of the 10 parameters used by Boltz will change the pump rates; therefore, the parameters have been highlighted in yellow on the main menu screen. The user can easily identify the factors affecting the pump rates and manipulate their values. The program asks the user if he wishes to calculate new pump rates between runs. If the user has not altered a highlighted variable, there is no need to recalculate the pump rates and the Boltz procedure can be bypassed. Bypassing Boltz saves considerable run time, especially if a large number of energy bins are used or many experiments are performed in succession.

The Boltz procedure was verified in the amplifier code by comparison with Honey's code. Identical values for the parameters used by Boltz were used in the amplifier code and Honey's model. The pump rates produced by *Boltz in* Honey's model and the amplifier model are identical for identical parameter sets. Several verification runs were performed over a large range of parameter values. In each case, both models produced the same pump rates.

Honey performed a thorough validation of his Boltz procedure. Since Boltz has been validated and returns identical values for a given parameter set in Honey's model and this amplifier model, the Boltz procedure is assumed to produce valid pump rates within the amplifier code. More discussion is included in the validation chapter.

2.3 Temperature Averaging of the Vibrational Modes

Stone's oscillator model includes a section of code that calculates the average vibrational temperatures of the CO_2 (100) and (001) modes during the pump pulse. This procedure was included in this amplifier model in order to provide a more accurate VT() array for use by Boltz.

The procedure relies upon the Boltzmann relation shown below.

$$\frac{n}{N_{CO_2}} = e^{(\frac{-h\nu}{k_B T})} \tag{2.2}$$

where

n = Population of the CO_2 (001) or (100) energy level

N_{CO_2} = Total population of CO_2 molecules

h = Planck's constant (J · seconds)

k_B = Boltzmann's constant (J · K)

ν = Characteristic frequency of the vibrational mode (seconds^{-1})

T = Characteristic temperature of the vibrational mode

Solving for T yields the following equation:

$$T = \frac{-h\nu}{k_B \ln(\frac{n}{N_{CO_2}})} \tag{2.3}$$

The average temperature is calculated by summing the values of T at each time step, then dividing by the number of time steps. The program is executed for three iterations of the pump pulse. A new VT() array is determined by the temperature averaging procedure after each iteration and is used by the Boltzmann pump rate procedure for the next iteration; three iterations are sufficient for convergence to accurate values of the vibrational temperatures used by the Boltz procedure.

2.4 Temperature Dependence of the Collisional Relaxation Rates

The procedure, TempDependence, was written to model the effect of temperature on the collisional relaxation rates, γ_a,γ_b,γ_c, and γ_{co}. The rates are modified in the procedure at each time step as the rate equations are solved. Physically, the rates increase because the temperature of the gas increases during pumping. The

physics forming the foundation of the procedure are sound; unfortunately the procedure code cannot be incorporated into the model since it produces invalid results. Further work can be done on this procedure to improve the model; the theoretical foundation of the procedure is explained below.

Some of the energy loaded into the cavity does not pump the gas mix; the energy merely increases the velocity of the molecules. Molecules collide with other molecules which results in an increase in the temperature of the gas mix. Part of the energy does succeed in pumping the CO_2 and N_2, but these molecules can also relax through collisions rather than through laser transition. Heat is released as the excited CO_2 and N_2 molecules fall to lower energy states through collisional relaxation.

The total energy in the system can be accounted for by summing the energy absorbed through successful pumping and the energy lost to heat as a result of molecular collisions.

Total Energy In = Pump Energy + Heat Energy

The temperature increase in the cavity is found by solving for the heat energy. The total heat energy into the system at any given time yields an increase in temperature expressed by the equation below.

$$\Delta T = \frac{E_{heat}}{N k_B C_v} \tag{2.4}$$

where

ΔT = Change in temperature
E_{heat} = Total heat added to the system through energy loading and collisions
N = Total number density of molecules in the cavity
k_B = Boltzmann's constant

C_v = Specific heat of the gases in the cavity

The collisional relaxation rates and number density of the (100) vibrational mode (n_b) increase with increasing temperature. Since collisions are more frequent, the number of (001) mode molecules (n_a) relaxing to the (100) level increases and the inversion is reduced. The equations describing the increase in the collisional relaxation rates and number density of the (100) mode are shown below.

$$\gamma_a = \gamma_{a_o}\sqrt{T/300}\; e^{\left(\frac{-h\nu}{k_B T - k_B 300}\right)} \tag{2.5}$$

$$\gamma_b = \gamma_{b_o}\sqrt{T/300}\; e^{\left(\frac{-h\nu}{k_B T - k_B 300}\right)} \tag{2.6}$$

$$\gamma_c = \gamma_{c_o}\left(\frac{T}{300}\right)^{3/2} \tag{2.7}$$

$$\gamma_{co} = \gamma_{co_o}\left(\frac{T}{300}\right)^{3/2} \tag{2.8}$$

$$n_b = n_b + n_{000}\; e^{\left(\frac{-h\nu}{k_B T}\right)} \tag{2.9}$$

where

T = The initial temperature of the gases plus $\Delta\, T$

n = The number density of the (100) or (000) vibrational level

The new values calculated for the relaxation rates and number density of the (100) vibrational mode (γ and n_b terms) are passed to the integration loop containing the rate equations. The (100) level molecular number density is increased by the rise in gas mixture temperature. The (001) level is essentially unaffected by temperature compared to the (100) level so its number density remains unchanged. Since the terms are altered according to the temperature of the gases at each time step, the rate equations incorporate the temperature dependence of the system.

The TempDependence procedure was not included in the model because it could not be properly validated. Validation is the most critical stage in model

development; if the model does not properly describe the system it is intended to model, it is not functional. The validation process is explained in the next chapter.

2.5 Addition of the Adams-Bashforth-Moulton Integrator

The Runge-Kutta integrator used in Gallagher's original code was replaced by an Adams-Bashforth-Moulton predictor-corrector method. The Runge-Kutta routine remains in the program and is used to determine three initial values needed to start the Adams-Bashforth-Moulton procedure. The predictor-corrector method runs faster than Gallagher's Runge-Kutta routine and produces more accurate results.

Stone's oscillator model also uses an Adams-Bashforth-Moulton integrator. The integrator used in this model (procedure ABMpc) is an adapted version of Stone's integrator. Stone developed his integrator using the algorithm in Burden's *Numerical Analysis* (1:221-223). Burden provides an excellent description of this multistep method.

The Adams-Bashforth-Moulton Predictor-Corrector procedure produces more accurate results, but is very sensitive to the time step parameter (h1). During the model's development, the algorithm would begin to oscillate wildly between predictions and corrections; eventually the program would fail due to an overflow of the exponential gain variable. The algorithm incorporates a time step constant established by the user. If this time step is above .04 for small input powers (e.g. a rectangular 80 MW input pulse), the procedure will fail. A time step of .02 or less is recommended for reliable and accurate output.

Unfortunately, a smaller time step results in longer run times. For an experiment with a duration of 25 lifetimes and time step of .02, the run time is approximately 12 minutes (using an 8 megahertz 80286 machine with a math coprocessor). The next chapter contains figures that show the model's percent error for time steps of .005 and .02.

2.6 *Amplifier Stringing*

The model uses several arrays to track the populations and output power and energy values during program operation. Experiments with long amplifiers (over 2 meters) and small time steps (.02) easily exceed the memory capability of 80286 machines with no augmented memory capability. Even though most personal computers will have in excess of 2 megabytes random access memory in the near future, this model was constructed to run on 80286 machines.

The model defeats the memory limitation by breaking up long amplifiers into a string of smaller amplifiers. Each amplifier in the string is .09 meters long. The user can model amplifiers which have a length equal to a multiple of .09 meters. The model automatically adjusts any input length to an integer number of .09 meter long amplifiers. (Figure 2.2). The input pulse that enters the original amplifier enters the

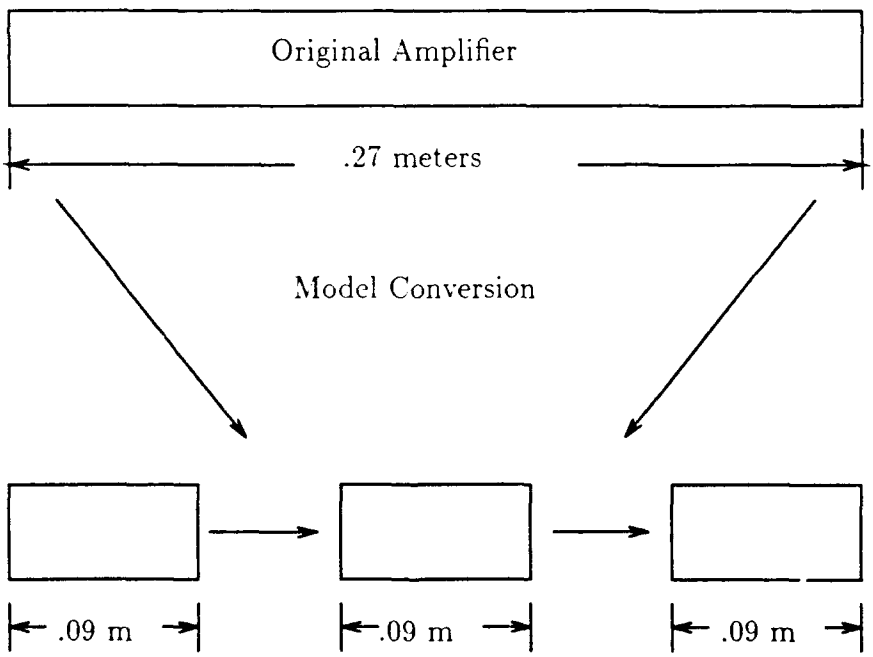

Figure 2.2. String of Amplifiers Sketch

first, .09 meter model amplifier and the output pulse data for this smaller amplifier is

written to the hard disk. The model then clears all the arrays and reads the previous output data file as an input file to the next amplifier in the string.

The delay in time for the pulse to travel from one amplifier to the next in the string is modeled by adding zeros to the front of the output pulse from the previous amplifier. For example, if the delay from one amplifier to the next in the string is equivalent to three integration time steps, then three zeros are written to the front of the input pulse before it is read by the second amplifier. Delay time is computed by dividing the amplifier length by the speed of light. The number of time steps (zeros) added to the front of the input pulse is calculated by the following equation:

$$Time\ Steps \;=\; \frac{Length}{h1\ tcav\ c} \tag{2.10}$$

Each amplifier in the string has a constant length of .09 meters. Parameter *tcav* is a normalization constant used to keep the values of program variables in the single precision range. Since the length is fixed at .09 meters and tcav = 2 x 10^{-8}, the number of time steps is dependent only on the integration time step selected by the user. For example, an integration time step (h1) of .005 yields exactly 3 time steps. Therefore, three zeros will be written to the front of the input pulse to simulate the delay time from amplifier to amplifier. A .02 integration time step yields a value of .75. The program uses the nearest integer value of the calculated time step. Since time steps are integer values, and the actual delay time based on the integration time step can be noninteger, some error can be induced in this process. The error caused by stringing a few amplifiers is less than when a large number of amplifiers are strung together. This is because the error is magnified by each amplifier in the series. The next chapter shows that this error is acceptable for amplifiers from .09 to 2.97 meters in length. A base length of .09 meters was chosen to keep the number of time steps exactly equal to 3 for an integration time step of .005.

The error could, perhaps, be reduced by dividing the amplifier into even lengths

with a last fractional length amplifier. For example, pulse travel time through an amplifier .48 meters long is exactly 4 time steps using a time step of .02 · tcav. An amplifier that is not an integer multiple of .48 would have a small fractional amplifier as the last amplifier in the string. The model would have to reinitialize the populations and conversion factors in addition to computing new pump rates. The complexity and longer run time associated with this option, along with the marginal gain in accuracy, make the method shown in Figure 2.2 more preferable.

III. Verification and Validation

The first step in the validation of a model is to verify that the code is executing as designed. Computer programs can easily contain bugs or programming errors. Obviously, a program that contains errors cannot be properly validated. An unverified model that produces near valid results is purely coincidental. Trying to determine the validity of an unverified model is a waste of time. Verification, determining that the model executes as intended, is necessary to prevent inaccurate validation.

Validation follows verification. Validation determines to what degree the model matches the real world process to the extent intended by the modeler. Both verification and validation will be discussed in this chapter.

3.1 Verification

The code was verified by analyzing the major procedures within the program. Instead of tracking the progress of each line, the procedures were verified at distinct positions within the code. QuickBASIC allows the programmer to step through the program one line at a time while displaying the values of up to six variables. Verification of each line is impractical in this model since there are over 2000 lines of code and over 50 variables. Verification of each line, although possible using the QuickBASIC editor, is not feasible given the time to complete this project.

Verification of the code at major junctions within the program is a feasible and acceptable technique. It is assumed that the code executes as intended between junctions if the values of the variables are correct at each junction.

The model was verified at the stages shown in Figure 3.1.

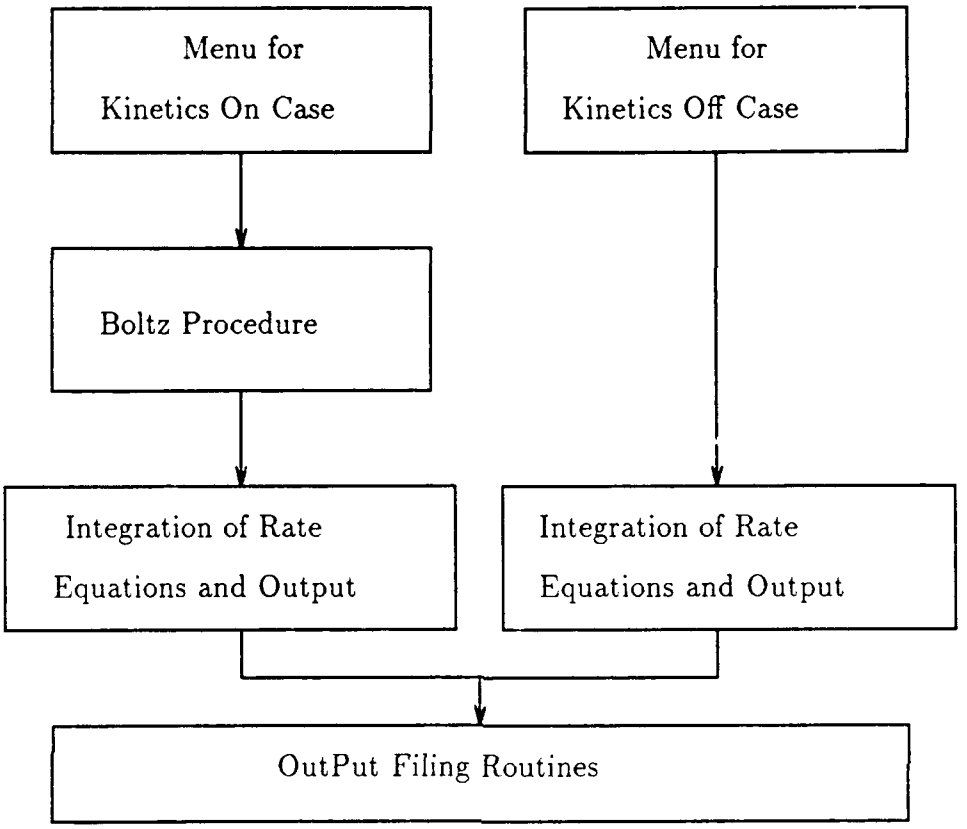

Figure 3.1. Flow Chart for Model Verification

Each block represents key points in the program that must run properly for the entire model to operate as intended. The verification of each block shown in Figure 3.1 is discussed in the following paragraphs.

Menus. The QuickBasic editor was used to verify the operation of the menus. The menus are critical to the program because they establish the values of the parameters used in the program. If a parameter value is not properly assigned while the user interfaces with the menu, then the model will not run properly. Essentially, the menus must run properly for the model to "start off on the right foot".

The menu screen for both the kinetics on and off cases was verified by assigning values to parameters through the menu and using the QuickBASIC watch option to check the value of the parameters during operation after the menu display. For

example, the values for the gas mix (%CO_2, %N_2, and %He) are assigned by the user while interfacing with the program through the menu. The user assigned values were compared to the values shown by the QuickBASIC variable watch feature. If the variable watch value equals the user specified value for every possible parameter, then the menu is working as intended.

Boltz Procedure. The Boltz procedure was verified by comparing the values returned by Boltz in this model with those returned by Boltz in Honey's model. The values of w_a, w_b, and w_c returned by Boltz in Honey's model were identical to the those for this model for several sets of input parameters. Therefore, Boltz works as intended in this model. Further, since Boltz was validated by Honey, the values produced by Boltz in this model are also valid.

Integration of the Rate Equations and Output. This amplifier model and Gallagher's model are almost identical for the kinetics off case. In both models, the pump rates and collisional relaxation rates are set to zero, and the user specifies a gain per unit length. The gain per unit length is used to determine the initial population of each cell. The difference between this model and Gallagher's model is the method of integration. Gallagher used a fourth order Runge-Kutta integrator; this model uses Runge-Kutta to produce initial values that are used by an Adams-Bashforth-Moulton predictor-corrector algorithm. For the purposes of verification, the output values for gain, populations, and power out should be similar in both models.

To verifiy the kinetics off case integration and output code, Gallagher's model and this amplifier model were run using identical parameter sets. Since Gallagher validated the kinetics off case by comparision to a Frantz-Nodvik solution (see reference (4)), if both amplifiers produce similar results, this model's integration procedure is verified. Validation at this stage is not assumed and its discussion is reserved for the validation section.

Several experiments were performed tc determine if the output of the Adams-Bashforth-Moulton integrator in this model matches the output of Gallagher's validated Runge-Kutta integrator. Table 3.1 lists the results of several experiments. In each experiment, the user specified gain per unit length and other parameters were identical for both amplifiers. Table 3.1 shows the output for both amplifiers under varying values of the user specified gain and amplifier length for a 10 MW input pulse. An integration time step of .04 was used for both amplifiers.

Table 3.1. Comparison of Runge-Kutta (R-K) and Adams-Bashforth-Moulton (A-B-M) Integrator Output for a 10 MW Pulse

Gain	*Amp.*	*R-K Integrator*			*A-B-M Integrator*		
	Len.	*Gain*	*Gain*	*Pwr*	*Gain*	*Gain*	*Pwr*
(%/m)	*(m)*	*1st Cell*	*Last Cell*	*Out*	*1st Cell*	*Last Cell*	*Out*
60	1	56.64	53.08	17.92	56.66	52.93	17.99
70	1	66.08	61.47	19.74	66.11	61.29	19.83
80	1	75.52	69.71	21.74	75.55	69.48	21.85
90	1	84.96	77.78	23.93	84.99	77.50	24.07
100	1	94.40	85.67	26.33	94.44	85.34	26.52
110	2	103.84	36.08	90.25	103.84	34.15	90.25
120	2	113.28	32.39	110.23	113.28	30.17	110.23
130	2	122.72	28.00	134.64	122.72	25.57	134.64
140	2	132.16	23.26	164.45	132.16	20.74	164.45
150	2	141.60	18.49	200.86	141.60	16.08	200.86

The table shows that the output of both amplifiers is essentially identical even though they use different integrators. Since Gallagher's integrator is verified and validated under the conditions shown in the table, the integrator of this model is working as intended.

Verification for kinetics on was performed in a manner similar to the kinetics off case. The code was executed for a given parameter set and the output was analyzed. Since Gallagher's amplifier model does not include the Boltz procedure for calculating the pumping terms, output for both models for given conditions is similar, but not

equal. Therefore, this amplifier's kinetics on case was compared to the kinetics off case. Gains and input powers for a 10 MW input pulse were compared to output pulse values for the kinetics off case using the same input pulse. For example, one run with kinetics on used a given parameter set and showed a 63.5694% gain in the amplifier as the input pulse entered the cavity. The resulting output was 17.6899 MW. The same gain was specified in this model using the kinetics off option and produced an output power of 17.1745 MW. Table 3.2 shows the kinetics on versus kinetics off values for different amplifier lengths.

Table 3.2. Comparison of Kinetics On and Kinetics Off Output for a 10 MW Pulse

Amplifier Length	*Kinetics On Output Pulse (MW) (Peak Value)*	*Gain %/m*	*Kinetics Off Output Pulse (MW) (Peak Value)*
1.0	17.6899	66.5694	17.6839
1.2	20.1971	66.5694	20.1902
1.4	23.4041	66.5694	23.2544
1.6	26.5693	66.5694	26.5651
1.8	30.3272	66.5694	30.3224
2.0	34.8945	66.5694	34.8945
2.2	39.8638	66.5694	39.8638
2.4	45.4898	66.5694	45.4898
2.6	52.0261	66.5694	52.0261
2.8	59.4350	66.5694	59.4350

Table 3.2 shows very reasonable values for the kinetics on case. The model's integrator is working as designed for both the kinetics on and kinetics off options.

The verification process to this point shows that the model's code works as intended. The menus provide the proper values of the input parameters to the program's main body. The Boltz procedure, already validated by Honey, provides exactly the expected pump terms for any set of input parameters. The Adams-Bashforth-Moulton integrator provides solutions to the rate equations that are ex-

pected for any given set of conditions; the solutions concur with values determined by an independent, verified and validated Runge-Kutta integration algorithm.

Output Filing. The output filing portion of the program writes data to files specified by the user. The user can choose to make a file of the populations, power output, energy output, gain, and input parameters. Verification of the output filing portion of the model was done by making runs, choosing a file option, and viewing the file using the DOS "TYPE" command. The model was operated and output files were selected for every available file option. The model output and files were identical for each file option.

The model's code executes each major task as designed. The menus assign values to the appropriate parameters, ensuring that the main body uses correct values. Boltz and the Adams-Bashforth-Moulton predictor-corrector return expected values for a given set of parameters. The output filing routines write the proper values to a storage file for a given menu choice.

The next step is to validate the model. The verification step only confirmed that the model operates as intended; verification does not prove that the working code accurately models reality. The next section discusses the validation process.

3.2 Validation

Validation was accomplished by comparing the model's output with a mathematical solution for amplifier gain under special conditions. Frantz and Nodvik derived closed form solutions to photon transport equations describing the growth of a pulse in a pulse laser amplifier (3:2346). Frantz and Nodvik account for the change in the inversion density between the front end of the pulse and the pulse's tail end.

The leading edge of the pulse encounters an initial, maximum inversion density. Photons in the tail end of the pulse encounter a reduced inversion due to the interaction of the leading edge with the inversion as the pulse entered the cavity. If

the pulse is strong enough, the leading edge can saturate the inversion and tail end photons may not encounter any inversion at all. In this case, the power into the amplifier at the tail of the pulse will equal the power out of the amplifier at the end of the pulse. Similarly, very small pulses experience a large inversion for the entire duration of the pulse since the amplifier is not saturated. Tail end photons interact with the inversion and the entire pulse is amplified.

Frantz and Nodvik provide a very useful equation for calculating the output pulse for a given input pulse in a simplified amplifier. They assume that the input pulse is square (constant amplitude) and the population inversion to be uniform throughout the medium (3:2347). The equation is written as follows:

$$n(x,t) = \frac{n_o}{1 - [1 - e^{(-\sigma \Delta_o x)}]e^{(-2\sigma\eta(t-x/c)/\tau)}} \tag{3.1}$$

where

$n(x,t)$ = Photon density at the amplifier exit at time t
n_o = Photon density of the input pulse
Δ_o = Population inversion as the input pulse enters the amplifier $(n_a - n_b)$
σ = Resonance absorption cross section (see equation 1.10)
x = Length of the amplifier
η = Total number of photons per unit area in the pulse
τ = Duration of the input pulse
t = Time since the pulse entered the amplifier
c = Speed of light

The equation calculates the photon density (power output) at the end of the amplifier from the moment the leading edge of the pulse exits the amplifier until the trailing edge of the pulse exits the amplifier. The equation does not model kinetics and is useful only for validation under specific conditions.

The Frantz-Nodvik equation ignores the dynamic processes that occur concurrent with the input pulse's entry into the amplifier. As the pulse travels through the

population inversion, collisional relaxation effects degrade the initial inversion. The inversion is degraded through collisional relaxation before the pulse can traverse the entire length of the amplifier. Frantz and Nodvik assumed that the leading edge of the input pulse encounters the same inversion during its entire trip through the amplifier. Since the equation ignores collisional relaxation, the relaxation terms in the model were not operating during validation.

The equation expresses the value that this model should calculate if one could use an infinite number of cells. The model's initial value for $n(x,t)$ at the amplifier's exit (power out) will always equal the Frantz-Nodvik solution for the front of the input pulse ($t = x/c$). Disregarding kinetics, the front end experiences the initial population inversion throughout the length of the amplifier. In a real world amplifier, kinetics are active continuously, even as the leading edge of the pulse propagates through the medium. Subsequent portions of the input pulse experience a depleted inversion. The model calculates the new inversion at each time step for each cell. Since the model calculates the gain for a number of cells where the inversion is constant for the length of each cell, the model's value for gain will not equal the Frantz-Nodvik solution. As the number of cells increases for a given amplifier length (achieved by lessening the time step), the gain will be calculated over a smaller Δ x and the model's output will more closely match the Frantz-Nodvik solution.

Several validation experiments were conducted for amplifiers with lengths between .09 and 2.97 meters. Experiments were conducted to compare the percent error between runs with differing numbers of amplifiers in the string (Figure 2.2) and different time steps. The number in the string is dependent on the amplifier length. The user explicitly chooses the time step. Percent error was calculated as follows:

$$\%\ Error \;=\; \frac{Frantz\ Nodvik\ Value \;-\; Model\ Value}{Frantz\ Nodvik\ Value} \cdot 100 \qquad (3.2)$$

3.2.1 Percent Error as a Function of Time Step Four validation runs were executed to compare the percent error for different time steps. Two input pulse durations were used to compare the percent error using a .005 and .02 time step. One pulse had a 40 nanosecond duration; the other pulse was 100 nanoseconds long. Figures 3.2 and 3.3 show the results of each run.

Figure 3.2 shows that the 40 nanosecond pulse did not have enough energy to saturate the inversion. If the inversion was saturated, the percent error would have approached zero at the end of the pulse. At saturation, power in equals power out and the error is zero. The curves for both time steps show that the inversion was not saturated because neither curve approaches zero at the end of the pulse.

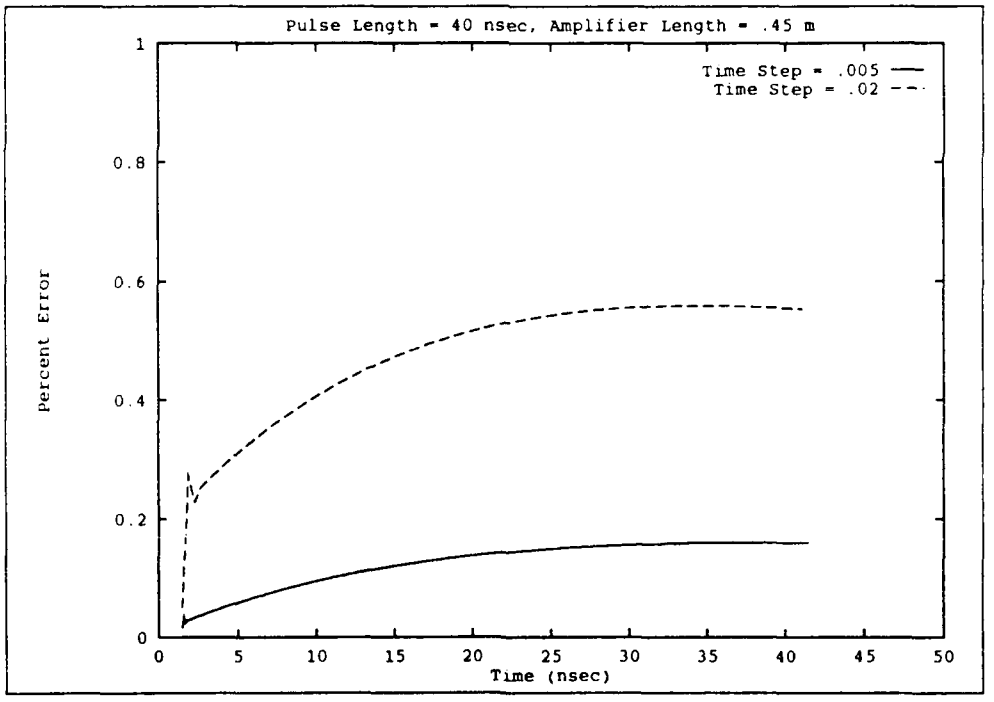

Figure 3.2. Percent Error Using a .005 vs. .02 Time Step (40 nsec pulse)

As anticipated, the % error is less when the user chooses a smaller time step. The peak error in Figures 3.2 and 3.3 is less than .6%. The curves suggest that the model will produce good results at either time step. The .02 time step produces less

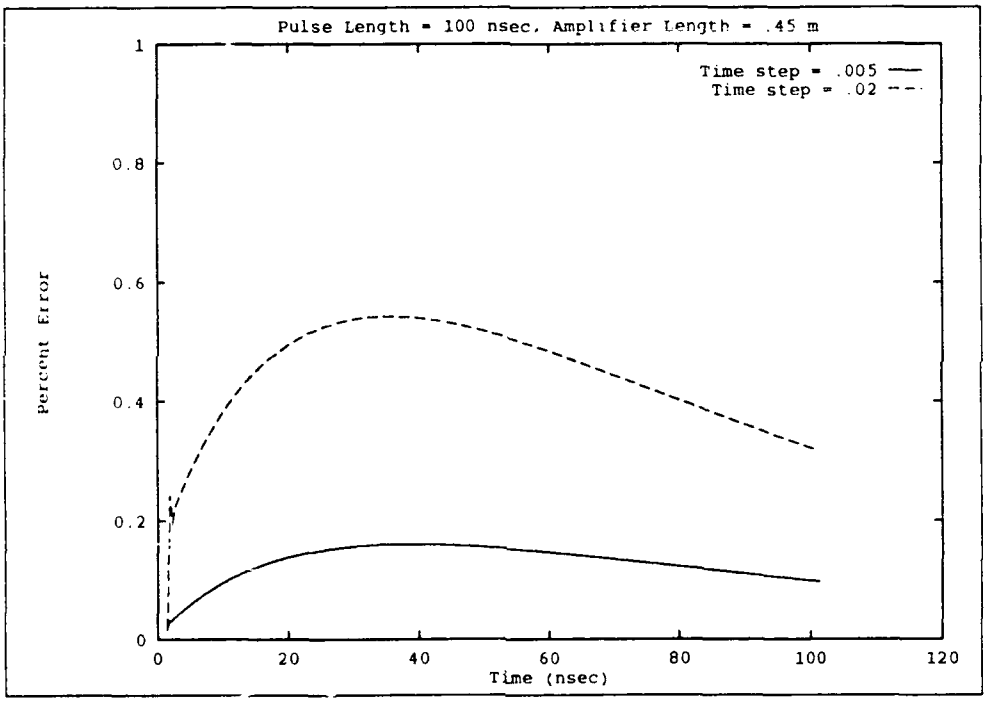

Figure 3.3. Percent Error Using a .005 vs. .02 Time Step (100 nsec pulse)

accurate results than the .005 time step, but the run time is shorter. A time step of .005 produces excellent results, but it can only be used to model pulses no longer than a few hundred nanoseconds. The combination of small time step and long pump and pulse time can easily cause the model to exceed the machine's random access memory.

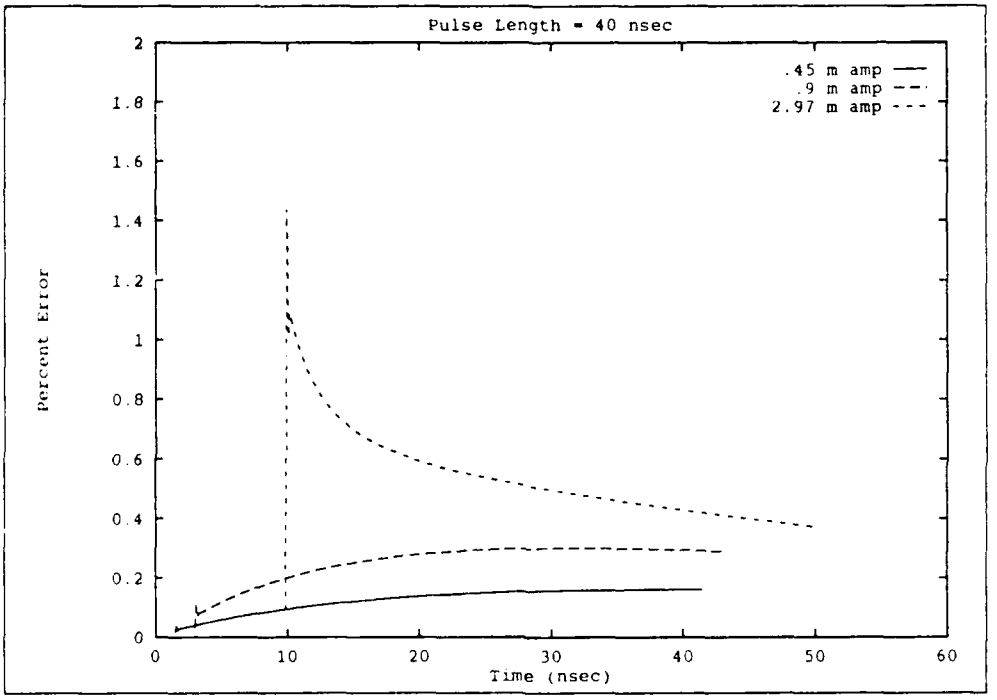

Figure 3.4. Percent Error for .45, .9, and 2.97 Meter Amplifiers (40 nsec pulse)

The 100 nanosecond pulse did come closer to saturating the inversion. Figure 3.3 shows that the error peaks about half way through the pulse and approaches zero near the end of the pulse. The 100 nanosecond pulse had more energy than the 40 nanosecond pulse and was able to drive the inversion closer to saturation.

Figures 3.2 and 3.3 confirm that the integrator is more accurate when using a smaller time step. Also, the 100 nanosecond pulse has less error at the end of the pulse than the 40 nanosecond pulse. This is expected since the longer pulse is more

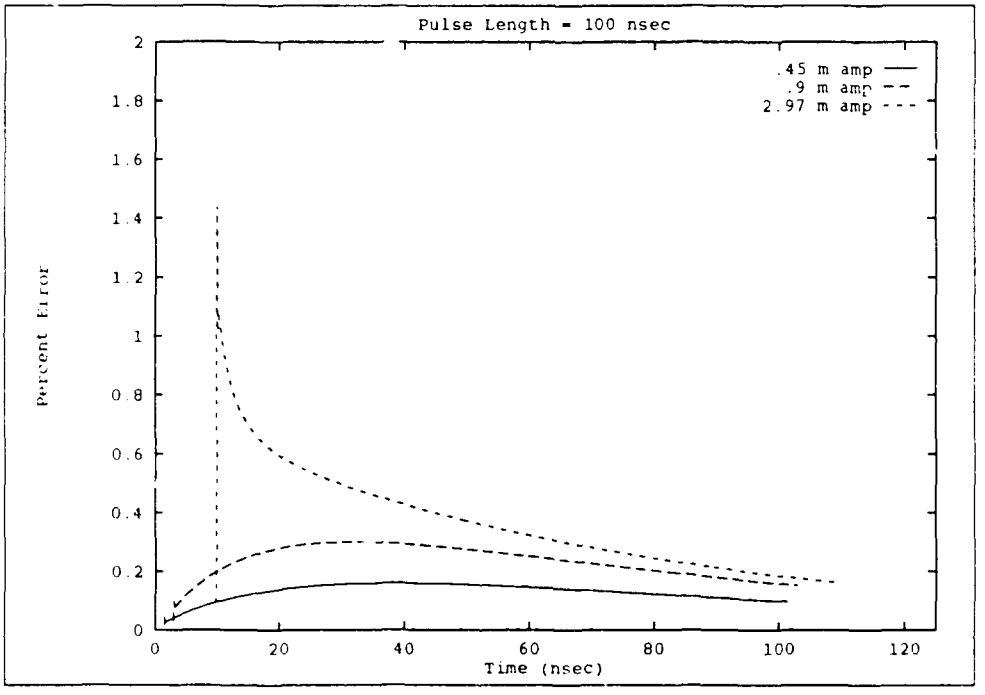

Figure 3.5. Percent Error for .45, .9, and 2.97 Meter Amplifiers (100 nsec pulse)

able to saturate the inversion. At saturation, model output and the Frantz-Nodvik equation equal zero.

3.2.2 Percent Error as a Function of Length Figures 3.4 and 3.5 show that error is magnified from amplifier to amplifier in the model string. The error induced in one amplifier is passed to the next amplifier. Subsequent amplifiers compound the error. The error increases from a peak error of .3% in a .9 meter amplifier to 1.5% in a 2.97 meter amplifier. A .9 meter amplifier is modeled by a 10 amplifier string and a 2.97 meter amplifier is modeled by 33 amplifiers. For an approximate 3 time increase in length, the model error is increased by a factor of 5. While this is a large increase, the overall error is still quite low.

As discussed above, the 100 nanosecond pulse drives the amplifier closer to saturation than the 40 nanosecond pulse. Hence, the 100 nanosecond curves have a more negative slope and are closer to 0% error at the end of the pulse. The spike for the 2.97 meter amplifier in Figures 3.4 and and 3.5 shows that the greatest error is induced at the front of the pulse when the medium is not saturated. At saturation, there is little error in each of the amplifiers in the string.

3.3 Conclusion

The model is valid under the special conditions assumed by Frantz and Nodvik. Disregarding kinetics, the model's output matches expected output with little error. The error that is present has expected values for specific times during the pulse. The error starts at zero as the input pulse encounters the initial inversion and approaches zero as the medium is saturated. The error between the initial pulse entry into the amplifier and saturation reaches a peak value and drops gradually as the inversion is gradually reduced.

Error is reduced by using a smaller time step. The Adams-Bashforth-Moulton integrator, like any numerical algorithm, produces more accurate results with a

smaller time step than with a large integration interval.

Error is magnified from amplifier to amplifier in the string. Output will be more accurate for shorter amplifiers since shorter amplifiers are modeled using fewer amplifiers in the string.

This model was only validated under the special conditions that accompany the Frantz-Nodvik equation. Obviously, the output should be compared to output from actual laser hardware if possible. The time available to complete this effort did not permit this type of validation.

The validation process not only determines how well the model represents reality, but assists in planning the experimentation strategy. Model experimentation was done with amplifiers less than three meters in length since validation showed that error increases with increasing length. Three meters is a substantial length for a space based laser amplifier. Experimentation is discussed in the next chapter.

IV. Results

Validation was performed for a specific set of input conditions. The input pulse was square and kinetics were not modeled. Actual laser pulses are not square. Stone's oscillator model produces data that simulates a real laser pulse. This model was constructed primarily to read in and amplify an output pulse from Stone's oscillator model. Although the model produces valid output when compared to the Frantz-Nodvik equations, it needs to be tested while serving its intended purpose. The comparison is not for validation, but to determine if the model provides results that are reasonable for a given set of conditions. The output could be not compared to data from actual amplifiers, so its accuracy could not be determined. The demonstrations described below were done to determine if the model reacts properly to changes in the various parameters (pressure, pump time, etc.). The scope of this work was limited to constructing and validating the amplifier model using the Frantz-Nodvik equation; a detailed analysis of its output is beyond the scope of this thesis. The number of different demonstrations that can be performed is infinite. For the purpose of this investigation, six were performed.

4.1 Model Experiments

Six experiments (demonstrations) were performed and their results analyzed. The following experiments were performed:

1. Amplify and produce an output pulse for a ^{12}C and ^{13}C based input pulse.
2. Compare the amplification of a ^{12}C input pulse using amplifiers with cavity pressures of 1, 2, and 3 atmospheres.
3. Compare the amplification of a ^{12}C input pulse using amplifiers with different cavity gas mixtures. One amplifier used an N_2:CO_2:He ratio of 20:10:70; the other used a ratio of 0:10:90.

4. Compare the amplification of a ^{12}C input pulse for different input times. One pulse entered the amplifier cavity after 100 nanoseconds of pumping. The other entered 140 nanoseconds after the amplifier started pumping.

5. Determine the peak $\frac{power\ out}{power\ in}$ and $\frac{energy\ out}{energy\ in}$ values for amplifiers of increasing pressures. The amplifier pressure was increased by .05 atmospheres from 1 to 3 atmospheres.

6. Determine the peak $\frac{power\ out}{power\ in}$ and $\frac{energy\ out}{energy\ in}$ values for amplifiers of increasing lengths. The amplifier length was increased by .09 meters from .09 to 2.97 meters. .09 meters is the length of the base amplifier used by the model.

Stone's oscillator model (version CO33G) was used to generate the input pulse. Table 4.1 lists the parameter values used to generate the input pulse. The same parameters were used to generate the ^{12}C and ^{13}C pulses.

Table 4.1. Oscillator Parameters Used to Generate the Input Pulse

Parameter	*Value*
Length	1 meter
Pressure	1 atmosphere
% CO_2, % N_2, % H_2O	10, 20, 70
Temperature	390 Kelvin
Integration Time Step	.01 Cavity Lifetimes
Cavity Lifetime	20 nanoseconds
Loss per Round Trip	3 %
Pump Pulse Length	20 Cavity Lifetimes
Energy Bins (Boltz)	35
Boltz Energy Range	5 ev
Tube Current Density	34 amps / cm^2
Energy Loading	99.74 Joules / liter
E/N	3 x 10^{-16} Volts $\cdot$ cm^2

Table 4.2 lists the parameters used in the amplifier for the conduct of the experiments. The amplifier parameters were kept constant with the exception of the

parameters dependent directly on the experiment being performed. For example, only the pressure was changed for experiments two and five; all other parameters retained the values shown in Table 4.2. This was done to maintain consistency between the experiments and served as a good check on the output of each experiment. For example, the ^{12}C output pulse in Figure 4.1 was constructed using the exact same amplifier and oscillator conditions as the 1 atmosphere pulse shown in Figure 4.2. As shown in the figures, each pulse reaches the same peak power output and has the same shape. This consistency aids in the evaluation of the results.

Table 4.2. Amplifier Parameters Used to Generate the Output Pulse

Parameter	*Value*
Input Beam Diameter	.05 meters
Length	.81 meters
Pressure	1 atmosphere
% CO_2, % N_2, % He	10, 20, 70
Temperature	300 Kelvin
Integration Time Step	.01 tcav
Normalization Constant (tcav)	20
Coupling Loss Term	1%
Loss per Unit Length	1%
Pump Pulse Length	5 tcav
Energy Bins (Boltz)	35
Boltz Energy Range	5 ev
Tube Current Density	68 amps / cm^2
Energy Loading	99.74 Joules / liter
E/N	3 x 10^{-16} Volts $\cdot$ cm^2

The normalization constant (tcav) shown in the table is used to keep the values in the computer code in the single digit range. Stone used the "cavity lifetime" in his oscillator model for the same purpose. Since this model must be compatible with Stone's model, this model uses the same normalization constants. The results of each experiment are explained in the following sections.

4.1.1 Experiment #1: Amplify a $^{12}CO_2$ and $^{13}CO_2$ Based Input Pulse Figure 4.1 shows the results of experiment number one. The peak power of the $^{12}CO_2$ input pulse is approximately 70 MW. The pulse is amplified to a peak power of approximately 105 MW. As expected, the output pulse is narrower than the input pulse. The sharper output pulse results from quick saturation of the amplifier inversion by the input pulse. The energy contained in the inversion is released in the form of the output pulse as the inversion is depleted by input pulse photons.

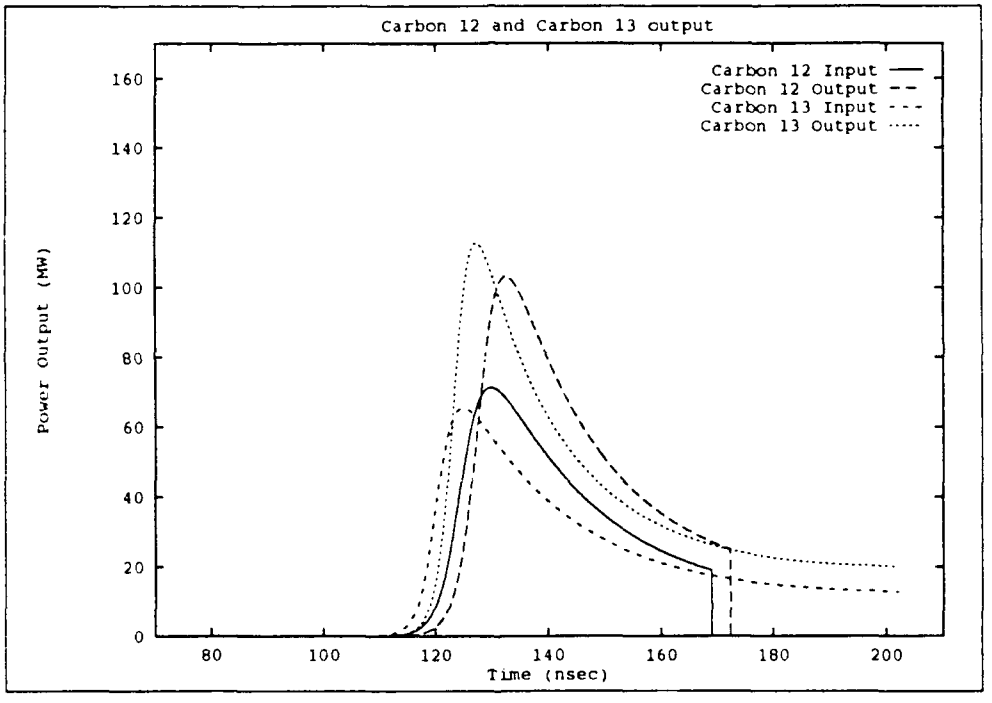

Figure 4.1. Power Output for Carbon 12 and Carbon 13

The model is applying a gain to the input pulse. The gain for a ^{12}C based CO_2 mixture should be less than that for a ^{13}C based CO_2 mixture because the Einstein A coefficient is greater for ^{13}C than for ^{12}C. The net result is that a ^{13}C pulse sees a greater inversion and is able to extract more energy in the form of an amplified input pulse. Figure 4.1 shows that the ^{13}C pulse experiences greater gain.

This first demonstration shows that the amplifier increases the power of the input pulse. Further, it shows that the model amplifies $^{12}CO_2$ and $^{13}CO_2$ based input pulses to differing degrees as one would expect. This demonstration does not prove that the value of the output is accurate since the results were not compared to laboratory data; however, it does provide output that is consistent with expectations (the pulse is amplified) and theory ($^{12}CO_2$ gain is less than $^{13}CO_2$ gain).

4.1.2 Experiment #2: Examine the Output Pulse for 3 Cavity Pressures Figure 4.2 shows that the output pulse peak power increases for increasing cavity pressures. The increase is accompanied by a narrowing in the pulse width. At higher pressures, the density of the inversion is greater. The input pulse meets a denser environment and forces more CO_2 (001) molecules to decay as it travels down the length of the amplifier. Again, model output agrees with expectations.

This behavior is beneficial to Doppler radar calculations. The narrower pulse provides more accurate range determination; higher powers extend the radar device's range. Current research is being done with higher cavity pressures in oscillators and amplifiers in order to sharpen the laser pulse and extend the useful range of the range/velocity finder.

4.1.3 Experiment #3: Examine the Output Pulse for 2 Gas Mixtures Figure 4.3 shows a dramatic difference in output power for a 20% N_2 mixture versus a 0% N_2 mixture. N_2 is used in CO_2 pulse lasers to aid in the pumping of CO_2 molecules to the (001) energy level. N_2 is easily pumped to an energy level that is only 18 cm^{-1} below the CO_2 (001) energy level. When N_2 is not present, the only pumping mechanism is collisional electron excitation. The result is a significantly lower CO_2 (001) density.

N_2 also aids in decreasing the lower level CO_2 (100) energy level, thus causing a greater inversion. The inversion is expressed as the difference between the number density of the CO_2 (001) and (100) energy levels ($n_a - n_b$). When N_2 is not available

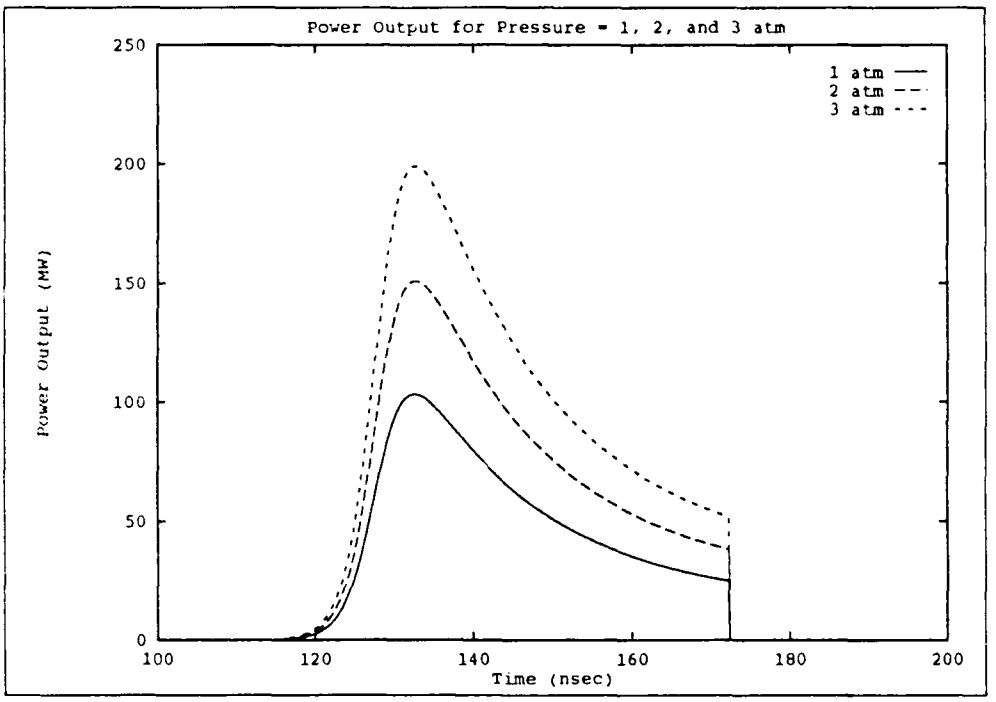

Figure 4.2. Power Output with Increasing Amplifier Pressure

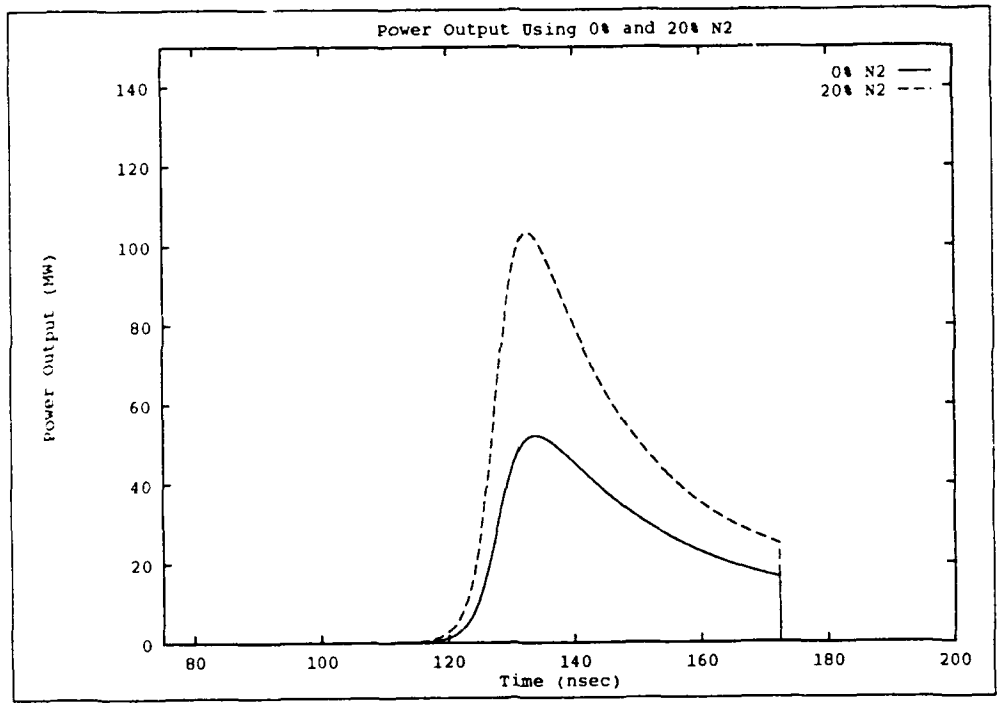

Figure 4.3. Power Output with 0% and 20% N2

to increase the (001) level or decrease the (100) level, the inversion will be much smaller. This concept is illustrated in Figure 4.3. The same input pulse is amplified much differently with and without the presence of N_2 in the amplifier cavity.

The output is consistent with expectations. N_2 is included as a component of the gas mixture to aid in establishing an inversion. One would expect that its absence would be marked by a decrease in the overall gain.

4.1.4 Experiment #4: Varying the Insertion of the Input Pulse Figure 4.4 shows the results of two different pump times. The pulse inserted after a 140 nanosecond pumping period is amplified more than the pulse inserted after 100 nanoseconds. This is because the amplifier is allowed more time to build an inversion. A longer pumping time results in greater pump terms (w_a, w_b, and w_c) returned by the Boltz procedure. The rate equations show that a greater value for the pump terms (caused by a longer pumping period) leads to a larger population inversion. The limit to the inversion is governed by the total number density in the gas mixture, collisional relaxation, and temperature effects. The rate equations predict that amplification will be greater for longer pump durations; Figure 4.4 shows that the model applies a greater gain to input pulses when the amplifier has been pumped for a longer period.

4.1.5 Experiment #5: Determine the peak $\frac{power\ out}{power\ in}$ *and* $\frac{energy\ out}{energy\ in}$ *values while increasing the cavity pressure.* Figures 4.5 through 4.7 show the effect of increasing pressure on amplification. Figure 4.5 shows an almost linear relationship between increasing pressure and increasing peak power output. Figure 4.5 reinforces Figure 4.2. Witteman ((16:60)) discusses the effects of increasing pressure on laser output. Pressure affects the following terms in the model: it increases the molecular number density; it increases the value of the pump terms; it increases the collisional relaxation rates; and it increases the value of the pressure-broadened linewidth ($\Delta\nu_p$). The increase in collisional relaxation and $\Delta\nu_p$ degrade the gain of the amplifier. The increase in the pump rates and the total molecular number density add to the gain

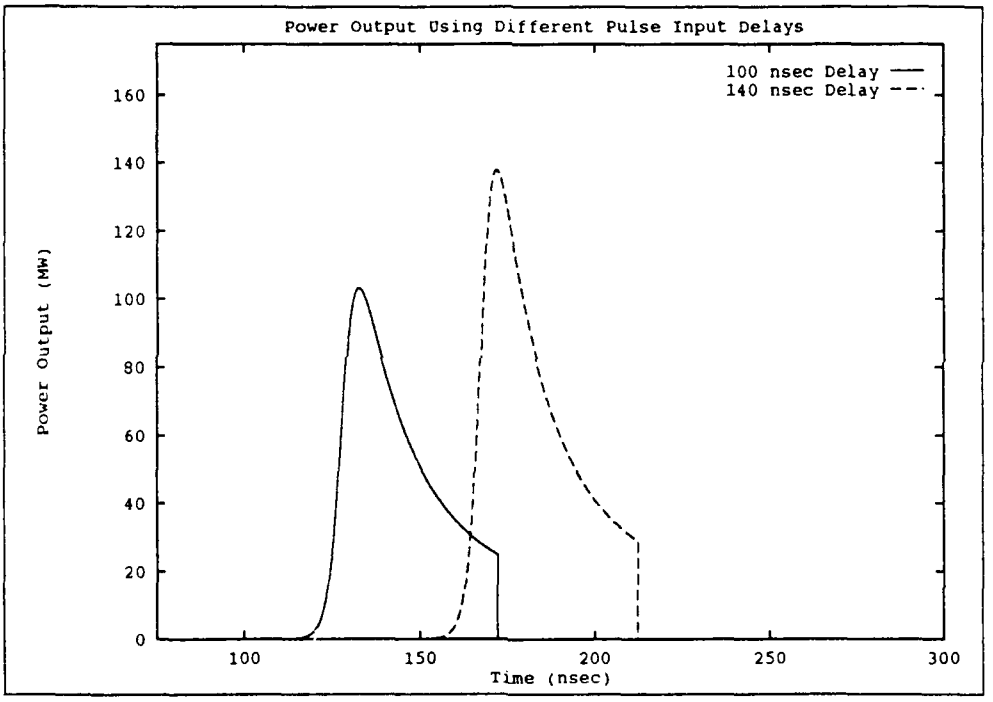

Figure 4.4. Power Output with 100 and 140 nsec Input Pulse Delay

and dominate the two degrading terms by a small margin. This is shown by the slight upturn of the curve at higher pressures. The slope of the increase reveals that it is beneficial to push laser development towards higher pressure amplifiers. A one atmosphere increase in cavity pressure can yield a twofold increase in energy out. Figures 4.6 and 4.7 show a linear relationship between pressure and energy or power. In laser radar applications, the energy of the beam is dissipated by 1/distance^2 to the target. Higher energies translate to longer ranges for a laser radar device. Considering the cost of placing any cargo in orbit, it is desirable to develop smaller, more efficient amplifiers for space laser radar applications. Increasing the amplifier cavity pressure is an excellent technique for achieving the desired performance. Unfortunately, the hardware associated with higher pressures tends to be heavy, and tradeoffs must be made in performance to satisfy weight constraints.

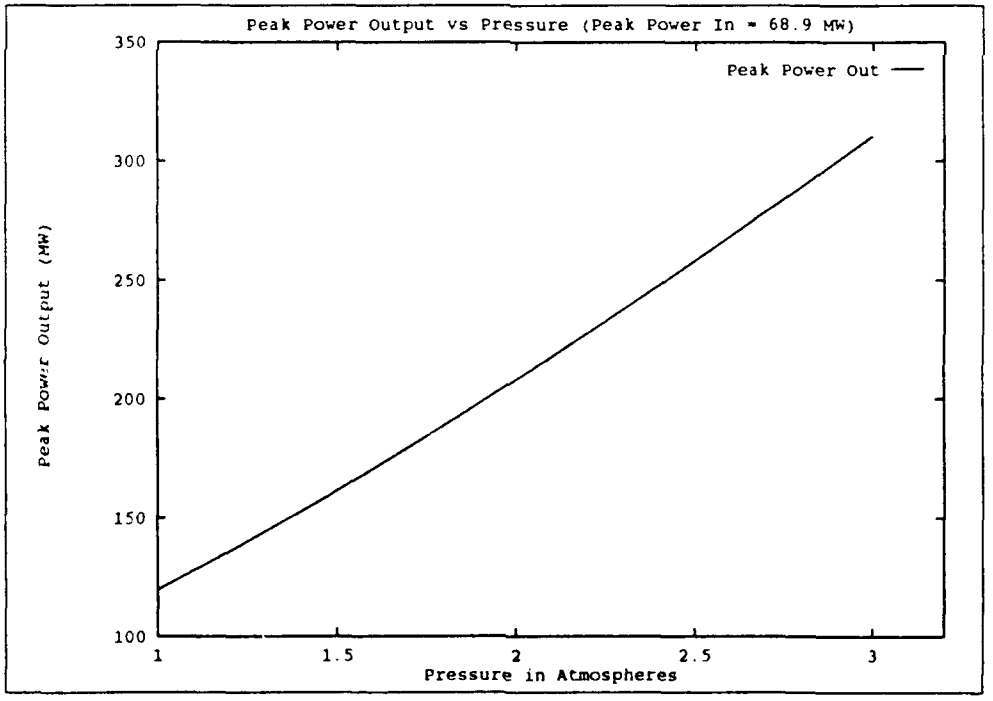

Figure 4.5. Peak Power Output with Increasing Amplifier Pressure

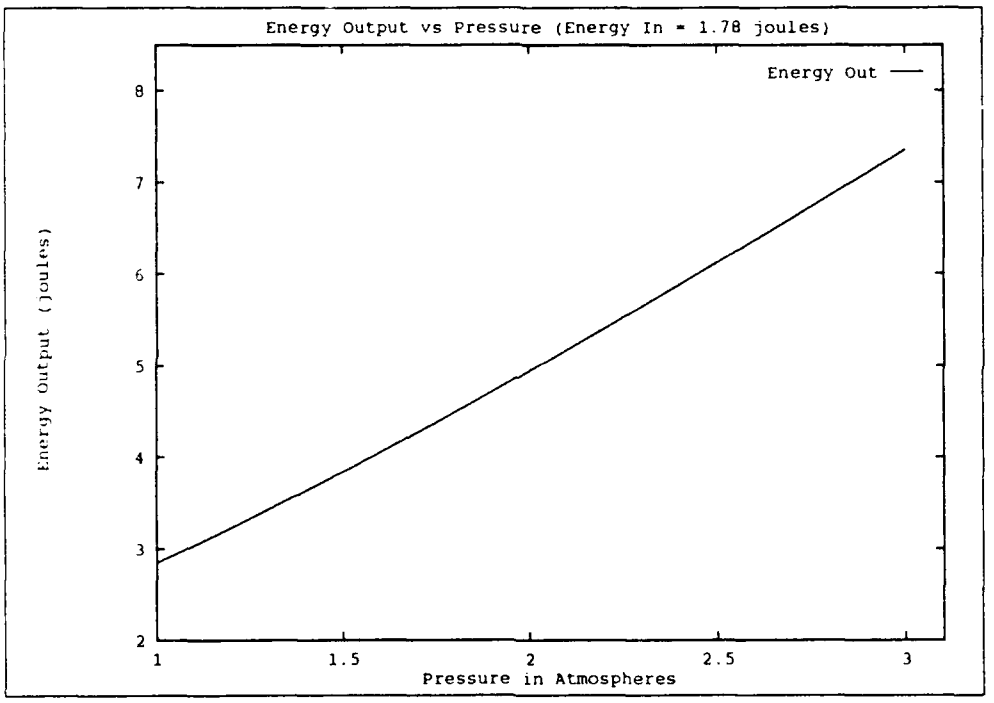

Figure 4.6. Energy Output with Increasing Amplifier Pressure

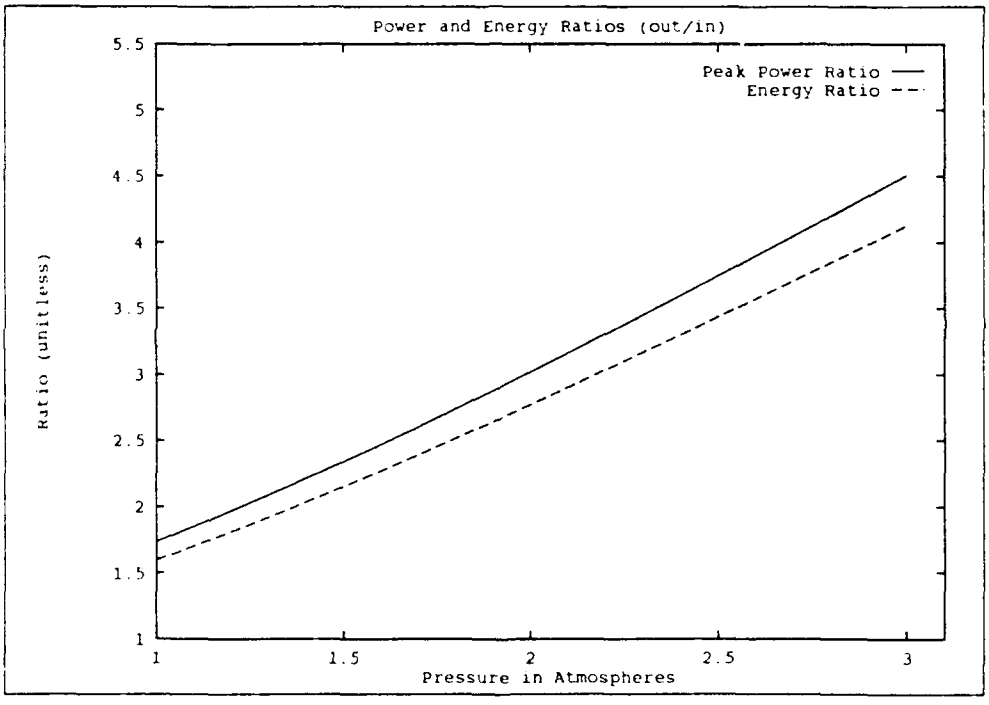

Figure 4.7. Power and Energy Ratios with Increasing Amplifier Pressure

4.1.6 Experiment #6: Determine the peak $\frac{power\ out}{power\ in}$ and $\frac{energy\ out}{energy\ in}$ values while increasing the amplifier length. Increasing the amplifier's length increases the resultant output power and energy. Since the input pulse is encountering a larger volume of excited CO_2 molecules, it extracts more energy from the inversion. Figures 4.8 through 4.10 show a slightly positive exponential increase in output power and energy for a given length of amplifier. For long or high power input pulses, the leading photons quickly saturate the inversion and the photons near the end of the pulse do not experience an inversion. For longer amplifiers, the same input pulse does not have enough energy to saturate the larger amplifier volume and more of the photons in the input pulse have an opportunity to strike an exited CO_2 molecule. Consequently, the peak power output will be greater.

The increase in power or energy from increasing the length does not benefit space operations. Cargo that is transported into low earth orbit must be as small and light as possible. Lengthening the amplifier is a brute force method of increasing the output for a given input. This technique is best suited for ground operations, such as an earth to space laser system.

4.2 Summary

The experiments discussed above were done primarily to observe the model's operation in conjunction with Stone's oscillator model. This purpose of this work was to create an amplifier model that is compatible with Stone's model; therefore, several runs were conducted to verify that it receives input and produces output that is logical for the given parameters. Each experiment produced trendwise consistent results for model input conditions. These experiments cover a very narrow range of all possible investigations in laser amplifier design; however, the fact that model output matches expected output reinforces the usefulness and face validity of the model. Further work with this model is warranted to determine if the model's output agrees with data from experiments with actual laser amplifiers.

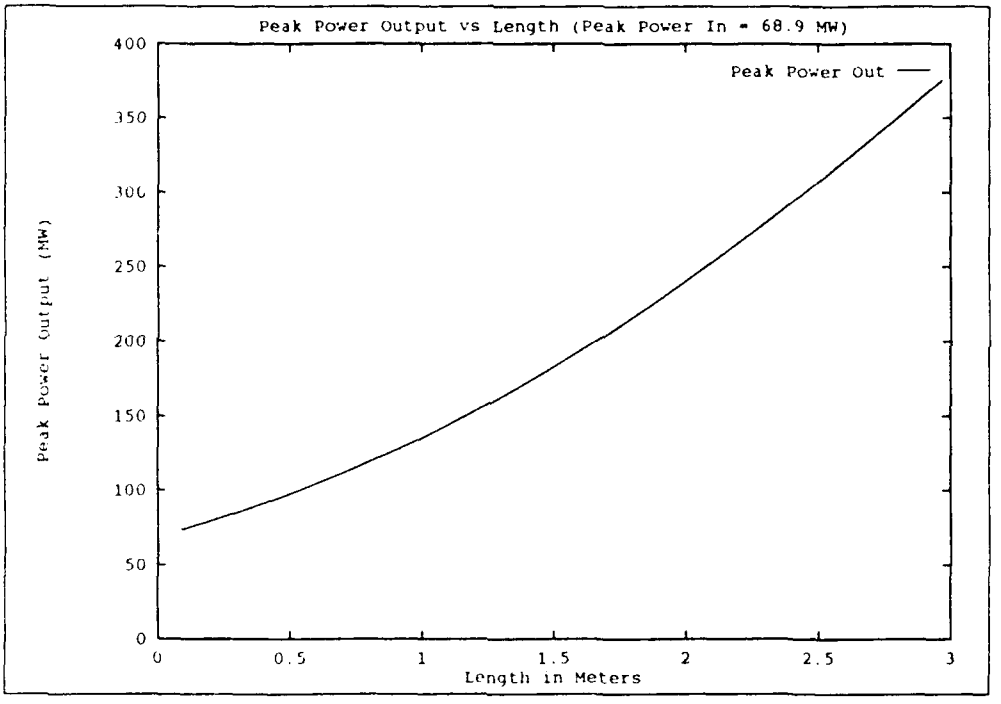

Figure 4.8. Peak Power Output with Increasing Amplifier Length

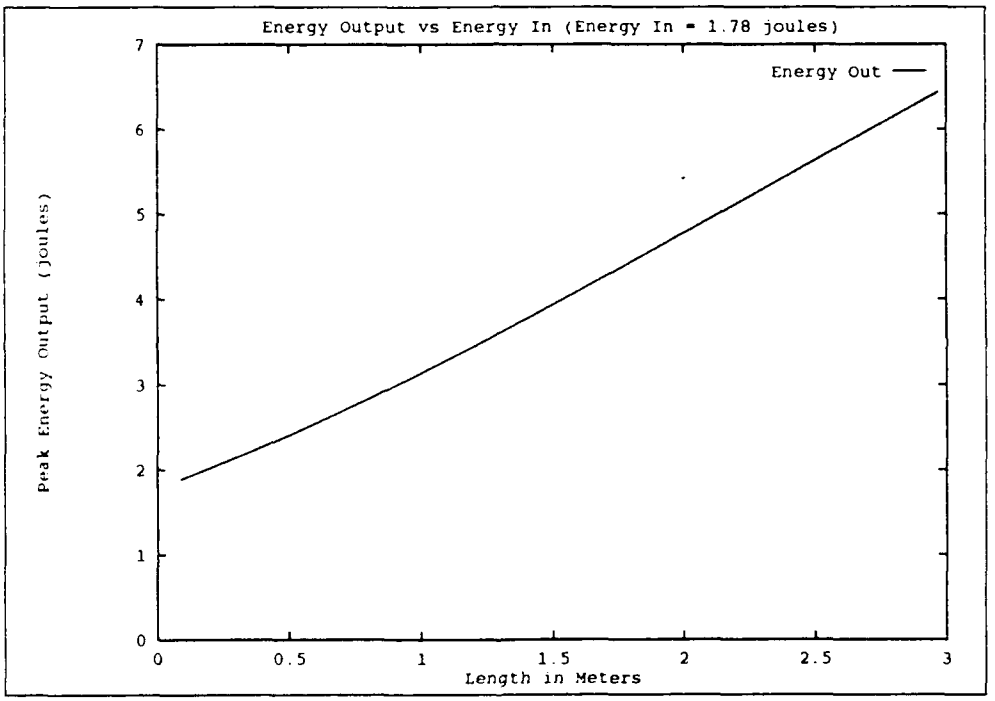

Figure 4.9. Energy Output with Increasing Amplifier Length

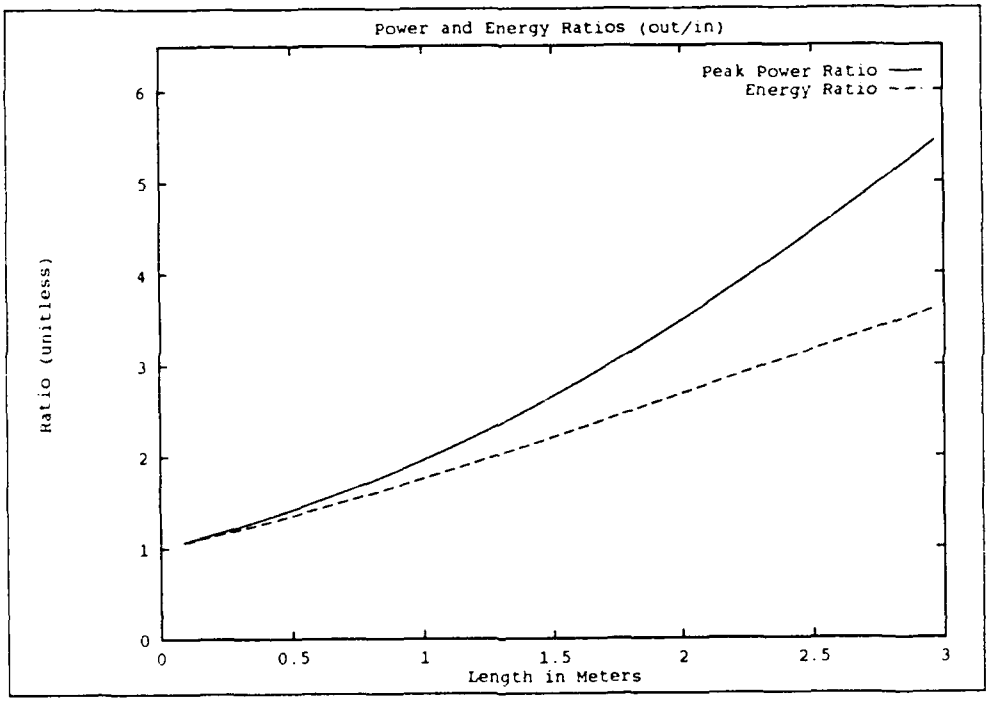

Figure 4.10. Power and Energy Ratios with Increasing Amplifier Length

V. Conclusion

With further laboratory testing, the model should prove to be a reasonable representation of a laser amplifier. Like any model, it has its strong points and weaknesses. This chapter outlines its advantages and limitations.

5.1 Model Advantages

The ultimate goal of this work was to improve Gallagher's amplifier model. This model surpasses Gallagher's model in several ways.

Gallagher's validated his model using the Frantz-Nodvik equation. Because his model does not incorporate amplifier stringing, he was limited by memory contraints to a minimum time step of .0416. The result is that peak error is close to 3% for the lowest possible time step. This model achieves percent errors below .4% for .9 meter amplifiers and is able to use a time step of .005.

Gallagher's model is length and time step limited. His model does not allow long lengths (above a few meters) and/or low time steps (below .04). Long lengths and short time steps cause his model to exceed the computer's memory capacity. This model defeats the memory limitations experienced by Gallagher through amplifier stringing. Time steps of .005 are possible for an infinite amplifier length. The program does not allow the user to input lengths greater than 2.97 meters, but this can easily be changed to include all possible lengths that are a multiple of .09 meters. The restriction to 3 meters only serves to prevent users from choosing a length that results in over a 60 minute run time.

This model uses the Boltz procedure to calculate more accurate values for the pumping terms shown in the rate equations. Gallagher's model calculates the pumping terms based on an assumed pump efficiency of the system. Since this model's rate equations have more accurate terms, the output is probably more accurate. Neither model has been compared to output generated by an actual amplifier.

Gallagher's model uses a slower, less accurate integrator. His Runge-Kutta routine runs slower and produces less accurate results than the Adams-Bashforth-Moulton integrator used in this model (1).

This model is more organized and easier to modify than Gallagher's model. Gallagher's original code contained fewer than seven procedures and a large main body. This model has over 22 procedures. These procedures allow the user to easily understand the code's structure and add embellishments as desired.

5.2 Model Limitations

The greatest limitation is the amount of memory consumed by the arrays. The model has a procedure which truncates the actual input pulse when small time steps (e.g .005) are used. The tail end of the pulse is not included in the run under these conditions. If the model is used on a machine with greater than 640 kilobytes of random access memory, truncation is not necessary.

The model can have excessive run times when modeling longer amplifiers. The run time is proportional to the length of the amplifier being modeled. The program takes roughly 2.25 minutes for each amplifier in the string after the pump rates are calculated. For example, for an amplifier length of .9 meters, the run time is 22.5 minutes using an 8 megahertz 80286 computer with a math coprocessor.

Since the Adams-Bashforth-Moulton integrator is time step sensitive, the model should be run using a time step value of .02 or less. Three iterations of the predictor-corrector are performed to make up for the inaccuracies caused by a time step of .02. More iterations translate to longer run times.

5.3 Conclusions and Recommendations

5.3.1 Conclusions This model is a significant improvement over the original model developed at the Air Force Institute of Technology. The percent error for amplifiers less than 3 meters long is less than 1/5 that of the original amplifier

model. The primary improvement is due to the addition of the Boltzmann and temperature averaging procedures which lead to a much more accurate calculation of the pump terms shown in the rate equations.

The model has potential for further embellishments, especially when used on a more capable machine than the 80286. Much of the software being written today is designed for more capable 80386 and 80486 machines.

The model is a good guide for the laboratory researcher to determine the effect of manipulating some of the parameters that affect the output of a laser amplifier. It can also be used in graduate level studies to reinforce classroom discussion of amplifier theory.

5.3.2 Recommendations The model does not need further embellishment to serve as a supplement to research or instruction in the classroom. It does have potential to model other aspects of input pulse amplification. The following recommendations list how the model can be improved:

1. Determine how to program temperature dependence into the model. This work considered the physics of temperature effects, but the process was not validated and more work could be done in this area.
2. Place more of the main body code into procedures. This effort made a great contribution in this area and the model is much more flexible and readable because of it. If further embellishments are to be made, the code must be readable by the programmer. The menus and output routines, as a minimum, can be placed into procedures.
3. Design a version of the code for use on more powerful machines. Although this is an easy programming task, the model would have to be revalidated. The goal should be to be able to run the code at a time step of .005 for a maximum simulation time of 500 nanoseconds.

4. Compare the output of this model with experimental data derived using actual laser amplifiers. The best way to validate a model is to compare its output with the output measured from an actual system.

These recommendations are feasible for a masters level graduate student.

Appendix A. *User's Guide*

This appendix provides a step-by-step explanation of how to use the amplifier model. The program does not have an on-line help (F1) feature, but it is simple to operate. The user should be familiar enough with the program after a few sample runs to use the model without this guide. This appendix should be read while running the program since it frequently refers the reader to the computer monitor.

The model can be used alone or in conjunction with Stone's oscillator code. In either case, the code is an executable file; the user does not need QuickBASIC 4.5 to run the model. Simply turn on the computer and insert the program disk into an available disk drive. Access the drive and type **Ampmodel**.

A.1 Overall Structure

Figure A.1 shows the model's overall structure. The model can amplify two types of input pulses. The user can create his own square (constant amplitude) pulse, or have the model amplify a pulse generated by Stone's oscillator model. The model's execution is the same for either type pulse once the user has initialized the amplifier's parameters (length, pump duration, etc.). The following sections walk the user through each of the stages shown in Figure A.1.

A.2 Cover Sheet

The cover sheet explains the modeled processes. This screen is a summary of the model's capabilities. Press any key to continue after you have finished reading the screen.

A.3 Data Files or Square Pulse Generation and Kinetics On/Off

This is where you decide whether you want to amplify a square input pulse (you will describe its amplitude and duration later) or a pulse created by Stone's

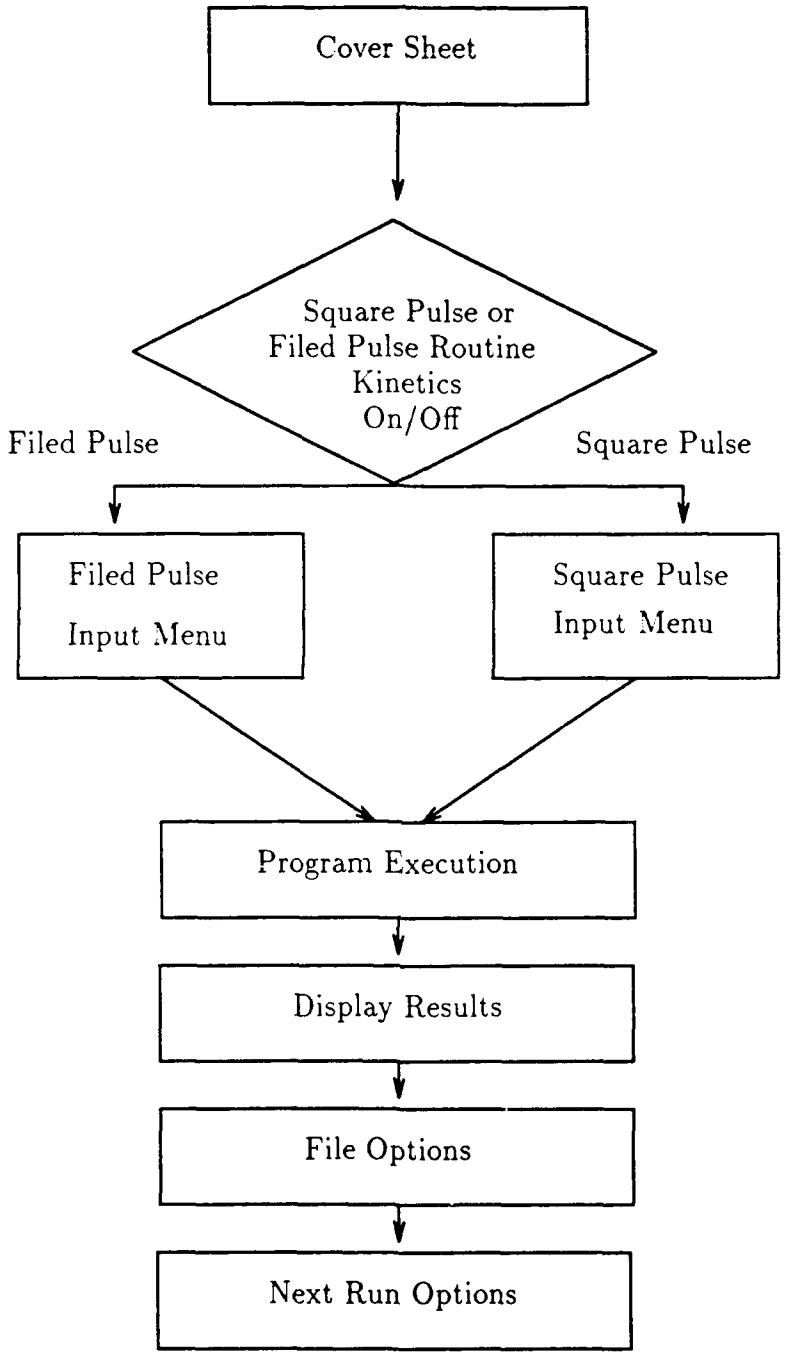

Figure A.1. Amplifier Model Structure

oscillator model. The model does not have a library of pulses from Stone's model, so you should have already created one. The model is able to receive pulses generated by Stone's oscillator model version CO33G. Decide which type of pulse you want to amplify (press **f** or **s**) and press **RETURN**.

You must now decide whether you want kinetics on or off. With kinetics on, the procedure BOLTZ will calculate the pumping terms based on parameters you set on an input screen shown later. If you choose kinetics off, the model will send you to the input menu, and prompt you for the gain per unit length during program execution.

The following two subsections describe both types of input pulses.

A.3.1 Data File Pulse Using a power data file created by Stone's program makes best use of this model since Stone's model produces a power file that closely resembles an actual laser pulse. The file pulse option can only be used if Stone's program was run with no time step change and the data was saved at every time step. Stone's model allows, and encourages, saving the output pulse power data at other than every time step. This model cannot input data from Stone's model unless there was a constant integration time step and every data value was saved.

Input the name of the data file at the **Input Filename** prompt. For example, type **c:myfile** if the data file is on the c drive. Press **RETURN** and an input menu will appear. The decisions you make here will determine the amplifier's performance and the duration of the run.

The user can change any lettered parameter on this screen. The default values shown are reasonable. The parameters shown in yellow affect the pump rates calculated by the BOLTZ procedure if you selected kinetics on.

The values chosen for the "Amplifier Length", "Maximum Run Time", and "Number of Energy bins" determine how long the model takes to run. The model uses a lot of memory in dynamic arrays whose size is dependent on the length, run

time, and number of energy bins. If the program fails during execution, it is because the machine ran out of random access memory. An error statement will appear with the following statement: **Press any key to return to the system.** Only users with 640 kilobyte random access memory machines may encounter memory problems. Failures are caused by a combination of a small time step, long run time, and large number of energy bins. Since the time step is set by the oscillator model for a filed pulse run, the user can reduce the maximum run time or number of energy bins. Keep the maximum run time below 25 for a time step of .02. If memory is exceeded with the lowest possible run time, reduce the number of energy bins to 30 or even 25 if necessary.

Press **RETURN** if the input parameters are correct for this run. If you want to run a square input pulse, press **q** and answer **y** to the **Go to Square Pulse Routine?** prompt.

A.3.2 Square Pulse Routine This menu is exactly the same as the file pulse menu, except you create a square pulse by adjusting the parameters shown in blue. The yellow parameters affect the BOLTZ pump rate procedure just like the file pulse routine. Pay particular attention to the time step, amplifier length, and number of energy bins input values if you are using a machine with limited memory. A time step of .02 provides excellent accuracy. Time steps above .04 may cause numerical instability of the program's integrator. Time steps down to .005 are possible if the maximum run time is low (200 nanoseconds). Users with extended memory machines (over 1 megabyte) can use a time step of .005 for longer durations, but the run time is longer. Press **RETURN** after the desired input parameters have been chosen.

A.4 Program Execution

A.4.1 Kinetics On The program will run and display the vibrational temperature values for the BOLTZ procedure if the user chooses kinetics on. The program

does three iterations of the BOLTZ procedure using the average vibrational temperatures of the CO_2 (001) and (100) energy levels during the pump pulse. These values are displayed to show their convergence to a given temperature dependent on the input parameters. A beep will sound and a prompt will appear when all calculations are complete and the model is ready to display the results of amplification. Press **RETURN** to continue at the prompt.

A.4.2 Kinetics Off A prompt will appear after completion of the input menu that asks for the **Gain per Unit Length**. Input any value greater than zero (100 is a good practice value) and press **RETURN**. The program then calculates the amplification based on your input gain. A beep will sound and a prompt will appear when all calculations are complete. Press **RETURN** to continue at the prompt.

A.5 Results

The first display is a graph of the input and output values over time. The limits of the plot can be changed by pressing **RETURN** and answering the prompts. To continue without adjusting the plots or after viewing adjusted displays, answer **n** to the **Plot with different limits?** prompt.

The next series of prompts asks if you want to view the populations or gain and energy output. Answer **y** or **n** as desired and a table of values will appear for the user specified time interval. If you are finished, answer **n** at the **Print again?** prompt.

A.6 File Options

If you want to make files of the populations, power output, gain, etc., press **y** at the **Make data files?** prompt. The menu is self-explanatory. You can make as many files as you wish and exit the file option by answering **n** at the **Make more data files?** prompt.

A.7 Next Run Options

The program issues several prompts to prepare for the next experiment. The first is the **Kinetics on (1) or off (0)** prompt. If you want the BOLTZ procedure involved in the next run, answer **1**.

The next prompt asks if you want to calculate new pump rates. If you do not plan on changing any of the parameters shown in yellow on the input screen, answer **n** and you will cut the run time in half for the next run. If you will make a change in a yellow parameter, you must answer **y** to achieve accurate output for the next experiment.

A.8 Conclusion

The model has many features and capabilities. This guide should be used to walk the user through a few experiments to become familiar with its operation. The user should find the model easy to use after a few experiences.

Bibliography

1. Burden, Richard L. *et al Numerical Analysis.* Boston: Prindle, Weber & Schmidt, 1978.
2. Dezenberg, George J. "Stable Lasers in Dynamic Environments," *Proceedings of SPIE—The International Society for Optical Engineering*, 783: 2-8 (19-20 May 1987).
3. Frantz, Lee M. and John S. Nodvik. "Theory of Pulse Propagation in a Laser Amplifier," *Journal of Applied Physics*, 34:2346-2349(1963).
4. Gallagher, Captain Frank Patrick. *Numeric Model of a CO_2 Laser Amplifier.* MS thesis, AFIT/GSO/ENP/89D-2. School of Engineering, Air Force Institute of Technology (AU), Wright-Patterson AFB OH, December 1989 (AD-A215 818).
5. Gilbert, J. *et al.* "Dynamics of the CO_2 Atmospheric Pressure Laser with Transverse Pulse Excitation," *Canadian Journal of Physics*, 50: 2523-2535 (October 1972).
6. Guy, S. R. and R. W. A. Coveney. "A Ground Based CO_2 Laser Doppler Velocimeter Employing an Offset Local Oscillator," *Proceedings of SPIE—The International Society for Optical Engineering*, 663: 182-186 (3-5 June 1986).
7. Honey, Capt David A. *A Numerical Solution to the Boltzmann Equation for Use in Calculating Pumping Rates in a CO_2 Discharge Laser.* MS thesis, AFIT/GEP/ENP/89D-5. School of Engineering, Air Force Institute of Technology (AU), Wright-Patterson AFB OH, December 1989 (AD-A216 376).
8. Moore, C. Bradley *et al.* "Vibrational Energy Transfer in CO_2 Lasers," *The Journal of Chemical Physics*, 46: 4222-4231 (June 1967).
9. Newman, L. A. *et al. CO_2 Laser Radar Source Program: Final Report*, August 1982 - September 1985. Report Number AFWAL-TR-85-1189. East Hartford CT: United Technologies research Center, July 1986 (AD-B106971L).
10. O'Shea, Donald C. *et al. Introduction to Lasers and their Applications.* Reading, Massachusetts: Addison-Wesley Publishing Company, 1978.
11. Pavlovskiĭ *et al.* "Experimental Investigation of Thermal Self-Interaction of Electron-Beam Controlled CO_2 Laser Radiation in a Master-Oscillator-Amplifier System," *Soviet Journal of Quantum Electronics*, 19: 998-1001 (August 1989).
12. Reilly, James P. "CO_2 Frequency Stable Amplifier Assessment," *Proceedings of SPIE—The International Society for Optical Engineering*, 783: 60-68 (19-20 May 1987).

13. Smith, Kenneth and R. M. Thompson. *Computer Modeling of Gas Lasers.* New York: Plenum Press, 1978.

14. Stone, David, Instructor, Department of Physics. Personal interview. Air Force Institute of Technology, Dayton OH, 1 April 1990 through 13 December 1990.

15. Willetts, David V. "How to Design Frequency Stable TEA CO_2 Lasers," *Proceedings of SPIE—The International Society for Optical Engineering*, 663: 132-135 (3-5 June 1986).

16. Witteman, W. J. *The CO_2 laser.* Berlin, West Germany: Springer—Verlag, 1987.

Vita

William Fredrick Anderson [redacted] He graduated from Irondequoit High School in Rochester, New York in 1976 and moved to Oneonta, New York to attend the State University of New York at Oneonta. A year later, he moved to West Point, New York to attend the United States Military Academy. He received a Bachelor of Science in Engineering in 1981. His assignments after graduation from the United States Military Academy include tours as a cavalry and infantry officer in Germany and as a staff officer in Korea. He entered the School of Engineering, Air Force Institute of Technology at Wright-Patterson Air Force Base, Ohio in May 1989.

[redacted]

REPORT DOCUMENTATION PAGE

Form Approved
OMB No. 0704-0188

1. AGENCY USE ONLY (Leave blank)	2. REPORT DATE	3. REPORT TYPE AND DATES COVERED
	December 1990	Master's Thesis

4. TITLE AND SUBTITLE
A COMPUTER MODEL OF A CO2 OSCILLATOR—AMPLIFIER SYSTEM

5. FUNDING NUMBERS

6. AUTHOR(S)
William Fredrick Anderson, Captain, USA

7. PERFORMING ORGANIZATION NAME(S) AND ADDRESS(ES)
Air Force Institute of Technology, WPAFB OH 45433-6583

8. PERFORMING ORGANIZATION REPORT NUMBER
AFIT/GSO/ENP/90D-01

9. SPONSORING / MONITORING AGENCY NAME(S) AND ADDRESS(ES)

10. SPONSORING / MONITORING AGENCY REPORT NUMBER

11. SUPPLEMENTARY NOTES

12a. DISTRIBUTION AVAILABILITY STATEMENT
Approved for public release; distribution unlimited

12b. DISTRIBUTION CODE

13. ABSTRACT (Maximum 200 words)

An existing CO_2 laser amplifier simulation model developed for use on IBM-compatible personal computers has been improved through the redesign and addition of supplemental procedures from several models. The models and selected procedures which form the basis of the improved model are described. One procedure calculates the pumping rates of CO_2 and N_2 through calculation of the Boltzmann equation. Another procedure calculates the average vibrational temperatures of CO_2's vibrational modes. A third procedure replaces the Runge-Kutta integrator used in the original model with a faster, more accurate Adams-Bashforth-Moulton predictor-corrector integrator. Model validation for special conditions along with sample output is then presented. A user's guide is attached as an appendix. The model allows students and designers to vary several input parameters to investigate the performance of the amplifier under various conditions. Parameters such as the cavity length, gas mix within the cavity, temperature, and pressure can be manipulated by the user in order to determine their effect on amplification.

14. SUBJECT TERMS	15. NUMBER OF PAGES
Carbon Dioxide; Laser; Amplifier; Model	85
	16. PRICE CODE

17. SECURITY CLASSIFICATION OF REPORT	18. SECURITY CLASSIFICATION OF THIS PAGE	19. SECURITY CLASSIFICATION OF ABSTRACT	20. LIMITATION OF ABSTRACT
UNCLASSIFIED	UNCLASSIFIED	UNCLASSIFIED	UL